http://doi.org/10.1093/plcell/koab283 THE PLANT CELL 2022: 34: 1745–1767

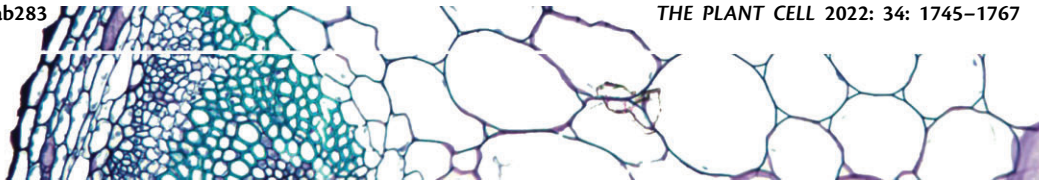

Research Article

Reduction of the canonical function of a glycolytic enzyme enolase triggers immune responses that further affect metabolism and growth in Arabidopsis

Leiyun Yang [1], Zhixue Wang [1], Aiqin Zhang [1,†], Ruchika Bhawal [2], Chunlong Li [3,‡], Sheng Zhang [2], Lailiang Cheng [3] and Jian Hua [1,*,§]

1 Plant Biology Section, School of Integrative Plant Science, Cornell University, Ithaca, New York 14853, USA
2 Proteomics and Metabolomics Facility, Cornell University, New York 14853, USA
3 Horticulture Section, School of Integrative Plant Science, Cornell University, Ithaca, New York 14853, USA

*Author for correspondence: jh299@cornell.edu
†Present address: Key Laboratory of Saline-alkali Vegetation Ecology Restoration, Ministry of Education, College of Life Sciences, Northeast Forestry University, Harbin 150040, China
‡Present address: Key Laboratory of Horticultural Plant Biology (MOE), College of Horticulture and Forestry Sciences, Huazhong Agricultural University, Wuhan 430070, China
§Senior author.

J.H. conceived the study; J.H. and L.Y. designed the experiments; L.Y., Z.W., and A.Z. conducted experiments; R.B. and S.Z. conducted HPLC-MS and its data analyses; C.L. and L.C. assisted the GC-MS analysis; L.Y. and J.H. wrote the manuscript with inputs from all other authors.
The author responsible for distribution of materials integral to the findings presented in this article in accordance with the policy described in the Instructions for Authors (https://academic.oup.com/plcell) is Jian Hua (jh299@cornell.edu).

Abstract

Primary metabolism provides energy for growth and development as well as secondary metabolites for diverse environmental responses. Here we describe an unexpected consequence of disruption of a glycolytic enzyme enolase named *LOW EXPRESSION OF OSMOTICALLY RESPONSIVE GENE 2* (LOS2) in causing constitutive defense responses or autoimmunity in *Arabidopsis thaliana*. The autoimmunity in the *los2* mutant is accompanied by a higher expression of about one-quarter of intracellular immune receptor nucleotide-binding leucine-rich repeat (*NLR*) genes in the genome and is partially dependent on one of these *NLR* genes. The *LOS2* gene was hypothesized to produce an alternatively translated protein c-Myc Binding Protein (MBP-1) that functions as a transcriptional repressor. Complementation tests show that *LOS2* executes its function in growth and immunity regulation through the canonical enolase activity but not the production of MBP-1. In addition, the autoimmunity in the *los2* mutants leads to a higher accumulation of sugars and organic acids and a depletion of glycolytic metabolites. These findings indicate that LOS2 does not exert its function in immune responses through an alternatively translated protein MBP-1. Rather, they show that a perturbation of glycolysis from the reduction of the enolase activity results in activation of NLR-involved immune responses which further influences primary metabolism and plant growth, highlighting the complex interaction between primary metabolism and plant immunity.

Received August 02, 2021. Accepted October 07, 2021. Advance access publication November 15, 2021

IN A NUTSHELL

Background: Plant NLR proteins are intracellular immune receptors that recognize pathogens and initiate defense responses against invaders. The expression of NLR genes is tightly controlled for effective defense as well as to balance defense and growth. To identify regulators of NLR gene expression, we performed a sensitized genetic screen and identified *LOS2* as a negative regulator of NLR gene expression and immune responses in *Arabidopsis thaliana*. *LOS2* encodes enolase, a key primary metabolism enzyme involved in glycolysis, and it was postulated to also encode a transcriptional repressor, MBP-1, via alternative translation initiation.

Question: The induction of immune responses by the *los2* mutation was unexpected, as primary metabolism is not generally viewed as having a negative impact on plant immunity. We wanted to find out whether the immunity connection made by the *los2* mutation was due to a defect in glycolysis or the transcriptional repressor MBP-1.

Findings: We found that the immunity regulation function of *LOS2* is through its enolase activity in glycolysis rather than MBP-1. Genetic elimination of the enolase catalytic activity but not the production of MBP-1 accounted for all defects observed in immunity and growth for the *los2* mutant. Perturbed glycolysis from reduced enolase activity triggers immune response accompanied by increase NLR expression. The heightened immune response also contributes to the reduced growth in the *los2* mutant, which was previously only attributed to a decreased primary metabolism. Not only is MBP-1 not involved in immunity and growth regulation, but it is also not detected under normal growth conditions. Interestingly, activated immune responses induce more accumulation of some primary metabolites such as sugars and organic acids, indicating a cross regulation between primary metabolism and immune responses.

Next steps: The next challenge is to find out the exact immune trigger(s) from the perturbed primary metabolism through multiple approaches such as metabolite profiling and genetic dissections. Further molecular links revealed will not only expand our understanding of immune response regulation but also provide potential molecular means for engineering plants with optimized growth and disease resistance.

Introduction

Plant primary metabolism generates energy, reducing equivalents and carbon skeletons which are not only essential for growth and development but also to fuel defense responses against pathogens (Bolton, 2009). Pathogen defenses in plants are carried out by a multi-layered immune system (Chisholm et al., 2006; Jones and Dangl, 2006). Intracellular nucleotide-binding leucine-rich repeat (NLR) proteins directly or indirectly detect effectors secreted from pathogens and mediate one of the critical layers of immune responses (Cui et al., 2015; Lolle et al., 2020). The recognition of pathogens triggers a diverse array of events including Ca^{2+} spikes, reactive oxygen species (ROS) burst, transcriptional reprograming of defense genes, and generation of defense phytohormones including salicylic acid (SA) (Buscaill and Rivas, 2014; Couto and Zipfel, 2016; Tang et al., 2017; Lolle et al., 2020). The immune signaling triggered by the activation of some NLR proteins requires the ENHANCED DISEASE SUSCEPTIBILITY 1 (EDS1)/PHYTOALEXIN-DEFICIENT 4 (PAD4) protein complex (Lapin et al., 2020) which also plays an essential role in boosting SA-related resistance programs (Cui et al., 2017). Primary metabolism has been shown to affect plant immunity via the production of primary metabolites. For instance, higher accumulation of sugars in leaves induces immune responses via interplay with phytohormones including SA (Bolouri Moghaddam and Van den Ende, 2012; Morkunas and Ratajczak, 2014; Trouvelot et al., 2014; Gebauer et al., 2017). Sorbitol in apple (*Malus domestica*) modulates the resistance to *Alternaria alternata* by regulating the expression of an *NLR* gene (Meng et al., 2018). More importantly, primary metabolism generates essential precursors to synthesize defense-related secondary metabolites including SA, pipecolic acid, and camalexin that have critical functions in plant immunity (Delaney et al., 1994; Glawischnig, 2007; Návarová et al., 2012; Shah et al., 2014; Piasecka et al., 2015). Therefore, primary metabolism plays a pivotal and often positive role in modulating immune responses.

Glycolysis is a central primary metabolic pathway conserved in almost all living organisms. The primary function of plant glycolysis is to oxidize hexoses to generate pyruvate, ATP, reductant as well as building blocks for a variety of amino acids, fatty acids, phytohormones, and secondary metabolites (Plaxton, 1996). Glycolysis is amphibolic and is able to utilize various low-molecular weight metabolites to generate hexoses including glucose and fructose via gluconeogenesis. Mutant plants with disrupted glycolysis pathway display drastic defects in growth and development such as stunted vegetative growth, distorted floral morphogenesis, reduced fertility, and dysfunction of guard cells (Rius et al., 2008; Prabhakar et al., 2010; Zhao and Assmann, 2011; Eremina et al., 2015), underscoring the essential function of glycolysis in plant growth and development.

Glycolytic proteins in nonplant organisms were reported to carry out versatile moonlighting functions in addition to their primary enzymatic functions, and their subcellular

localizations determine which functions they execute (Pancholi, 2001; Kim and Dang, 2005; Boukouris et al., 2016; Didiasova et al., 2019). For instance, glyceraldehyde-3-phosphate dehydrogenase in human acts as a glycolytic enzyme in cytosol but is a component of transcriptional coactivator complex regulating expression of a histone gene *H2B* (Zheng et al., 2003). Also, the mammalian α-enolase (*ENO1*) gene encodes an enolase that catalyzes the conversion of 2-phophoglycerate (2-PG) to phosphoenolpyruvate (PEP) in cytoplasm, while its alternative translation product c-Myc Binding Protein (MBP-1) acts as a transcriptional repressor of the c-*myc* gene in the nucleus (Ray and Miller, 1991; Feo et al., 2000; Lung et al., 2010). Although moonlighting functions of glycolytic proteins are common in non-plant organisms (Rodríguez et al., 2001; Zheng et al., 2003; Shams et al., 2014; Boukouris et al., 2016), these functions are rarely reported in plants.

One enolase protein in *Arabidopsis thaliana* has been suggested to have such a moonlighting function. Arabidopsis has three enolase (*ENO*) genes, two of which (*ENO1* and *ENO2*) encode proteins with demonstrated enolase activities (Andriotis et al., 2010). ENO1 functions in plastids while ENO2 is cytosolic and accounts for the majority of enolase activities throughout plant development (Andriotis et al., 2010). The loss-of-function *eno1* mutations or overexpression *ENO1* does not confer measurable defects (Andriotis et al., 2010), while knockdown mutants of *ENO2* display multiple growth and developmental defects such as reduced shoot and root growth (Eremina et al., 2015). These biochemical and genetic studies indicate that ENO2 is the predominant enolase essential for plant growth and development. The *ENO2* gene has also been implicated in plant abiotic stress responses. *ENO2* is also known as *LOW EXPRESSION OF OSMOTICALLY RESPONSIVE GENE 2* (*LOS2*) because the *los2-1* mutant was isolated based on having a low expression of the abiotic stress response gene *RD29A* in the Arabidopsis C24 accession (Lee et al., 2002). The *los2-1* mutant is hypersensitive to freezing stress (Lee et al., 2002) and salt stress (Barkla et al., 2009) compared to the C24 wild-type (WT) plants. By analogy to its mammalian homolog *ENO1*, the Arabidopsis *LOS2* gene was postulated to encode two proteins, the full-length isoform enolase (named as ENO2 herein) and the N-terminal truncated isoform MBP-1, via distinct translational initiation sites (Kang et al., 2013). The *LOS2* function in abiotic stress response was hypothesized to result from the transcriptional repressor activity of MBP-1 or the proposed moonlighting function of enolase as a transcriptional repressor. Recombinant ENO2 protein was shown to bind in vitro to the promoter sequences of *ZAT10*, which is a negative regulator of the cold-responsive gene *RD29A*, and the *los2-1* mutant has a higher expression of *ZAT10* compared to the C24 WT plant (Lee et al., 2002). Additionally, plants that carry the transgene coding for MBP-1 under the strong CaMV 35S promoter exhibit hypersensitivity to ABA (Kang et al., 2013; Liu et al., 2017) and osmotic stress (Kang et al., 2013). However, the MBP-1 protein was not easily detected in plants, and this was attributed to proteasomal protein degradation (Kang et al., 2013). Interestingly, plants overexpressing MBP-1 exhibit stunted growth, reduced fertility, decreased expression of endogenous *LOS2* transcripts, and reduced enolase activity similarly to the loss-of-function *los2* mutants (Kang et al., 2013; Eremina et al., 2015). It was proposed that *LOS2* gene alternatively translates MBP-1 to repress its own expression to maintain enolase homeostasis (Eremina et al., 2015). Despite the study of the effect of MBP-1 overexpression, the existence and function of endogenous MBP-1 have not yet been determined.

In this study, we found an unexpected role of the enolase coding gene *LOS2* in repressing plant immunity, and we further investigated the contribution of the canonical function of enolase and the putative endogenous MBP-1 to the role of *LOS2* in growth, development, and immunity. We found that the *los2* mutants exhibited enhanced disease resistance and autoimmunity, which were largely dependent on NLR and SA signaling. Genetic elimination of the potential production of the MBP-1 protein did not yield measurable effect on plant growth or immunity, while the long-form ENO2 alone accounts for the full LOS2 function observed. In addition, the MBP-1 protein could not be detected from the *LOS2* gene under conditions used in this study, and it could be detected at a very low level when sequence encoding only MBP-1 was expressed under the strong 35S promoter. Therefore, MBP-1 is unlikely a bona fide alternative translation product of the *LOS2* gene under normal growth conditions. Furthermore, site-directed mutagenesis of a conserved amino acid critical for enolase activity could not recue any of the *los2* mutant defects examined, supporting that canonical enolase activity of ENO2 mediates all roles of *LOS2* in growth and immunity. Our study strongly indicates the use of enolase function of the *LOS2* gene in regulating growth, development, and immunity in Arabidopsis and highlights the large effect that perturbation of glycolysis has on growth and environmental responses, both directly and indirectly.

Results

A *smo3/los2* mutation constitutively activates immune responses

We sought enhancer mutations for immune responses via a sensitized genetic screen using the *bon1 mos1* mutant. The loss-of-function mutant *bon1* displays autoimmunity phenotypes due to the elevated expression of an NLR gene *SUPPRESSOR OF npr1-1, CONSTITUTIVE 1* (*SNC1*) (Yang and Hua, 2004), and the *mos1* mutation restores the *SNC1* expression to the WT level and suppresses autoimmunity of *bon1* (Bao et al., 2014). An ethylmethylsulfonate mutagenesis screen was performed to identify suppressor mutations that restored autoimmunity to the *bon1 mos1* mutant, and those mutated alleles were named as suppressor of *mos1 bon1* (*smo*) (Yang et al., 2020). The *smo3* mutation was one of the mutations identified; and the *bon1 mos1 smo3* triple

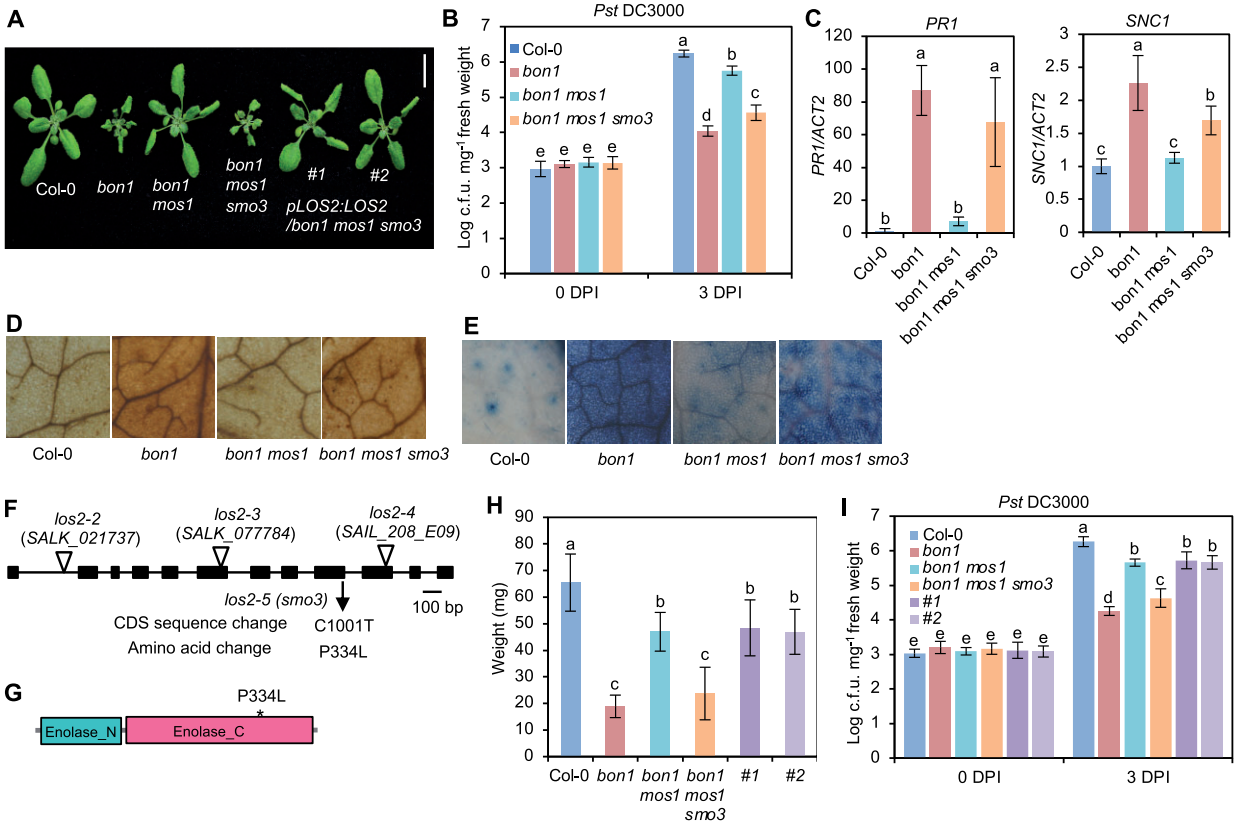

Figure 1. A mutation in *LOS2* constitutively activates immune responses. A, Morphology of Col-0 WT, *bon1*, *bon1 mos1*, *bon1 mos1 smo3*/*los2* and two representative complementation lines of *pLOS:LOS2* in *bon1 mos1 smo3* (#1 and #2). Scale bar = 1 cm. B–E, Growth of bacterial pathogen *Pseudomonas syringae pv. tomato* (*Pst*) DC3000 (B), analysis of *PR1* and *SNC1* gene expression (C), DAB staining (D), and trypan blue staining (E) in Col-0, *bon1*, *bon1 mos1*, and *bon1 mos1 smo3*/*los2*. F, Position of the point mutation generated from the ethylmethylsulfonate screen and T-DNA insertion mutations in *LOS2*. The position of T-DNA insertions was adapted from Eremina et al. (2015). G, Predicted functional domains of LOS2 protein by SMART. * indicates *smo3*/*los2-5* mutation. H and I, Quantification of weight (H) and growth of bacterial pathogen *Pst* DC3000 (I) in Col-0, *bon1*, *bon1 mos1*, *bon1 mos1 smo3*, complementation lines #1 and #2. $N \geqslant 23$ for (H). Six biological replicates were performed for (B) and (I). Three biological replicates were performed for (C). Error bars represent standard deviation (SD). Different letters indicate significant difference tested by one-way ANOVA/Duncan's multiple range test via R 3.6.3 with "agricolae" package, $P < 0.05$.

mutant was significantly smaller than *bon1 mos1* mutant (Figure 1, A and H). In addition, the triple mutant displayed enhanced disease resistance to a virulent bacterial pathogen *Pseudomonas syringae pv. tomato* (*Pst*) DC3000 compared to *bon1 mos1* mutant (Figure 1B). Also, under nonpathogenic conditions, the *bon1 mos1 smo3* mutant had increased expression of *PR1* (a defense response marker gene) and *SNC1*, as well as accumulation of H_2O_2 and cell death as compared to *bon1 mos1* mutant (Figure 1, C–E). These results indicate that *bon1 mos1 smo3* is an autoimmune mutant, and the *smo3* mutation constitutively activates immune responses in the *bon1 mos1* mutant.

Using Mapping by Sequencing (Zhu et al., 2012; Hua et al., 2017) on the F2 population of a *bon1 mos1 smo3* and *bon1 mos1* cross, we localized the *smo3* mutation to the *LOS2* gene (Figure 1F), and the resulting proline-334-to-leucine change was in the C-terminal enolase domain of LOS2 (Figure 1G). To verify that *SMO3* is *LOS2*, a WT genomic fragment of *LOS2* (*pLOS2:LOS2*) was transformed into *bon1 mos1 smo3* mutant for complementation test. The majority of the T1 plants showed the *bon1 mos1* mutant phenotype, and co-segregation of the *bon1 mos1*-like plants with the transgene was observed in all six independent T2 lines analyzed (Figure 1, A and H). In addition, these complementation lines were more susceptible to *Pst* DC3000 compared to *bon1 mos1 smo3* mutant, at a similar level to the *bon1 mos1* mutant (Figure 1I). These results confirm that *LOS2* is *SMO3* and that a nonsynonymous mutation in *LOS2* activates immune responses in the *bon1 mos1* mutant background.

los2 mutants have autoimmune responses

We further characterized the disease-resistance phenotype of the *smo3*/*los2* single mutant, which is hereafter designated as *los2-5*. At 3 days after inoculation, the growth of the virulent pathogen *Pst* DC3000 was about 10 times lower in the *los2-5* mutant compared to the Col-0 WT, indicating an enhanced disease resistance in the mutant (Supplemental Figure S1A). Even in the absence of pathogen infection, the *los2-5* mutant already had elevated expression of *PR1*, suggesting a defense response induction (Supplemental Figure S1B). These analyses

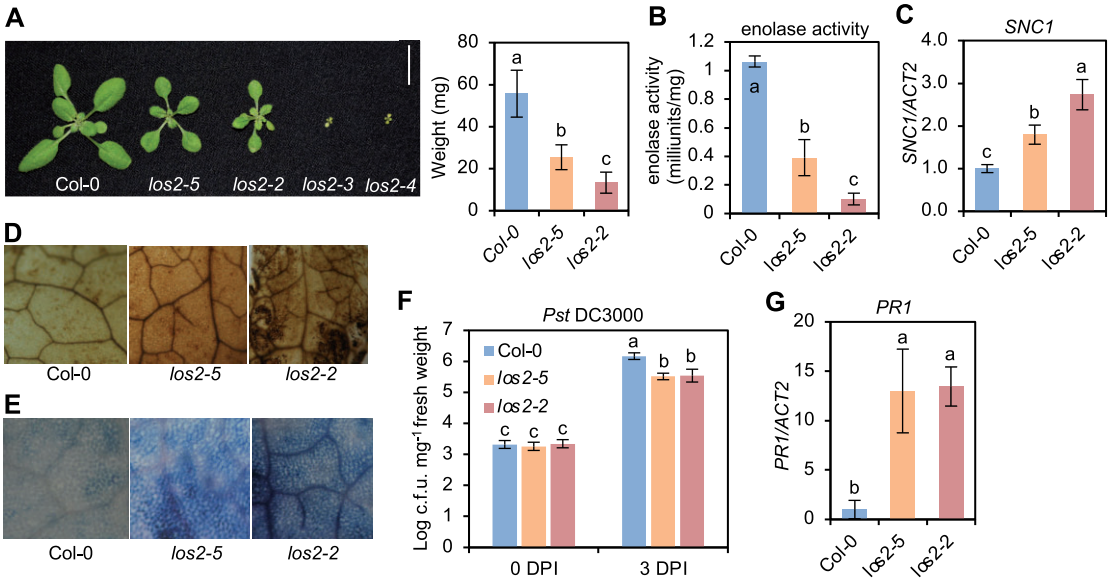

Figure 2 The *los2* mutants display constitutively activated immune responses. A, Morphology of Col-0, *los2-5*, *los2-2*, *los2-3*, and *los2-4* mutants, and quantification of weight of Col-0, *los2-5*, and *los2-2*. Scale bar = 1 cm. $N = 20$. B–G, Enolase activity (B), analysis of *SNC1* gene expression (C), DAB staining (D), trypan blue staining (E), growth of bacterial pathogen *Pst* DC3000 (F), and analysis of *PR1* gene expression (G) in 2-week-old WT, *los2-5*, and *los2-2*. Four biological replicates were performed for (B). Three biological replicates were performed for (C) and (G). Six biological replicates were performed for (F). Error bars represent SD. Different letters indicate significant difference tested by one-way ANOVA/Duncan's multiple range test via R 3.6.3 with "agricolae" package, $P < 0.05$.

indicate that *LOS2* is a negative regulator of plant immunity and that the *los2-5* mutant exhibits autoimmunity, or upregulated immune responses in the absence of infection. Because the *los2-5* mutant had a weaker growth defect than *bon1 mos1 los2* (Figures 1, A and 2, A) and *bon1 mos1* has a residual autoimmunity, it is likely that the *los2* defect is independent and additive with defects of *bon1 mos1*. Therefore, the *bon1 mos1* mutant provided a sensitized background for isolating weak autoimmune mutants, which has been seen in another *SMO* gene *HOS15* (Yang et al., 2020).

The *LOS2* gene has been studied previously for its role in abiotic stress tolerance but has not been characterized in the context of biotic stress responses. We therefore examined three previously reported *los2* mutants in the Col-0 background for their immune phenotypes. The *los2-2* (SALK_021737) contains a T-DNA insertion in the first intron (Figure 1F) which results in reduced *LOS2* transcript accumulation and reduced enolase activity compared to WT (Eremina et al., 2015). Both the *los2-3* (SALK_077784) and *los2-4* (SAIL_208_E09) alleles, with T-DNAs inserted in exons (Figure 1F), have even lower enolase activities compared to the *los2-2* mutant (Eremina et al., 2015). We found that the enolase activity in the *los2-5* mutant isolated in this study was reduced to 37% of the WT level, to a less extent as compared to the *los2-2* mutant which had 10% of WT enolase activity (Figure 2B; Supplemental Figure S1C). Correlated with the strength of the molecular defects of *LOS2* mutations, *los2-5*, *los2-2*, and *los2-3*/*los2-4* had increasingly stronger growth defects. Both *los-5* and *los2-2* had smaller rosette size and exhibited early flowering compared to WT with these defects stronger in *los2-2* (Figure 2A; Supplemental Figure S1D). Additionally, the *los2-2* mutant had shorter siliques (Supplemental Figure S1E) similarly to previously reported (Eremina et al., 2015), and accumulated less chlorophyll compared to WT (Supplemental Figure S1F). These two defects were not observed in the *los2-5* (Supplemental Figure S1, E and F) but were attributed to the defect of the *LOS2* gene (see later result), further supporting *los2-2* being a stronger allele than *los2-5*. The other two alleles, *los2-3* and *los2-4*, exhibited more severe defects in growth and development than *los2-2* (Eremina et al., 2015; Figure 2A). They were extremely tiny and were not able to set seeds in standard growth conditions. Therefore, we utilized *los2-5* and *los2-2* for further analyses.

Both the *los2-5* and *los2-2* mutants exhibited autoimmunity. They had increased expression of *SNC1* and accumulated more H_2O_2 and cell death as compared to WT in the absence of pathogen infection, while the *los2-2* mutant had a stronger effect as compared to the *los2-5* mutant (Figure 2, C–E). The *los2-5* and *los2-2* mutants also had elevated resistance to *Pst* DC3000 as compared to WT; and the level of increase of resistance was similar in the two mutants (Figure 2F). In addition, both mutants showed a similar fold increase in the expression of *PR1* compared to the WT (Figure 2G). Taken together, these data indicate that *los2-2* mutant is a stronger allele in growth and development than *los2-5* mutant while the increase of disease resistance compared to the WT is comparable between these two mutants.

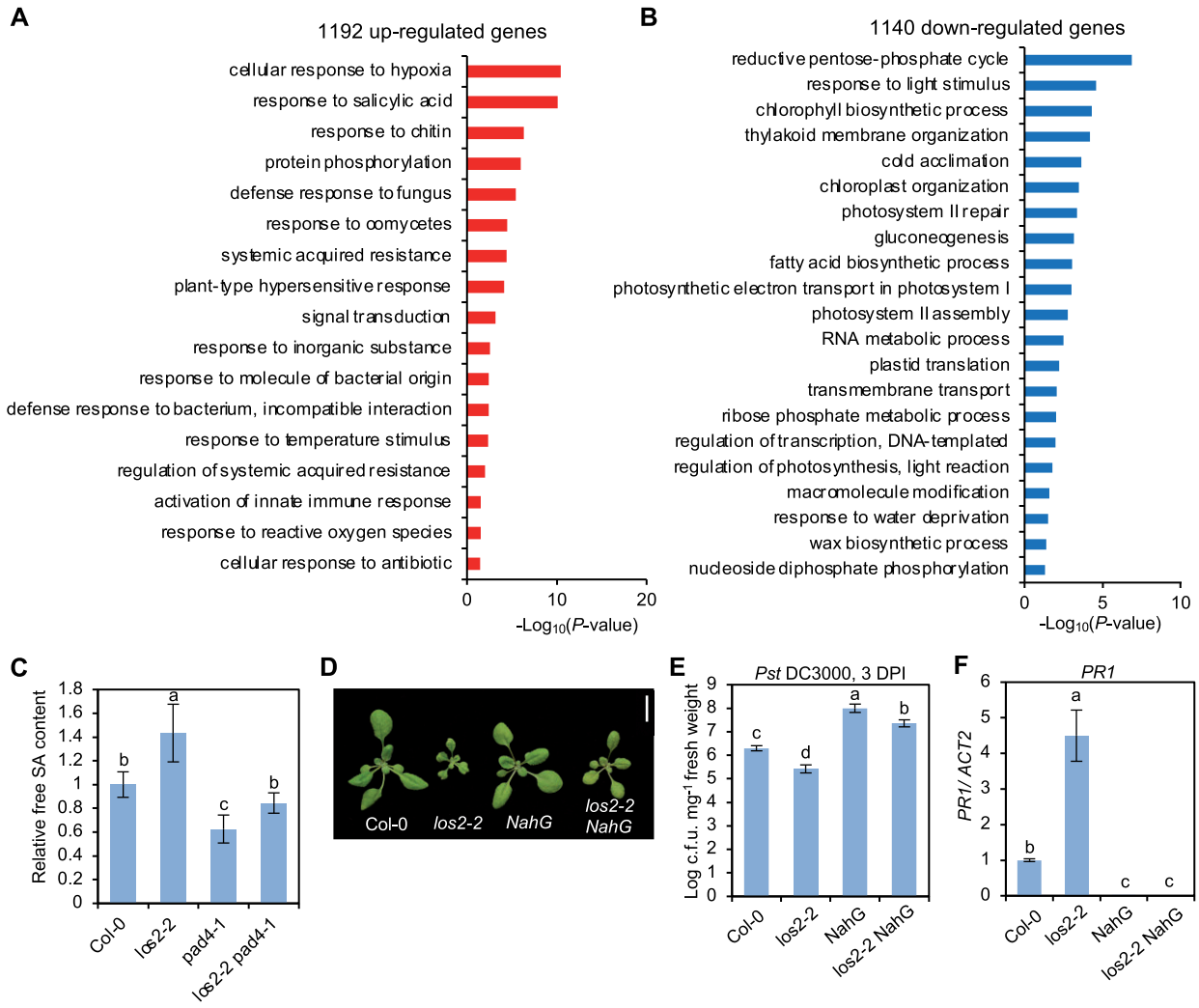

Figure 3 The activated defense responses in *los2* mutants are dependent on salicylic acid pathway. A and B, GO enrichment analysis of 1192 upregulated genes (A) and 1140 downregulated genes (B) in *los2-5* mutant as compared to WT. Enriched GO terms were identified by Panther (https://www.arabidopsis.org/tools/go_term_enrichment.jsp). C, Relative amount of free SA in Col-0, *los2-2*, *pad4-1* and *los2-2 pad4-1*. The amount of salicylic acid in Col-0 was set to "1." Five biological replicates were performed. D, Morphology of Col-0, *los2-2*, *NahG* and *los2-2 NahG*. Scale bar = 1 cm. E and F, Growth of bacterial pathogen *Pst* DC3000 (E) and analysis of *PR1* gene expression (F) in Col-0, *los2-2*, *NahG* and *los2-2 NahG*. Six and three biological replicates were performed for (E) and (F), respectively. Error bars represent SD. Different letters indicate significant difference tested by one-way ANOVA/Duncan's multiple range test via R 3.6.3 with "agricolae" package, $P < 0.05$.

Defense-related genes are upregulated in the *los2* mutant

To investigate how *LOS2* influences plant immunity, we carried out transcriptomic analyses of the *los2-5* mutant and Col-0 WT by mRNA sequencing (RNA-seq). Two-week-old shoots were sampled with three biological repeats for RNA extraction and subsequent sequencing. Differentially expressed genes (DEGs) between *los2-5* and the WT were selected with false discovery rate (FDR) set at less than 0.05. The *los2-5* mutant had 1192 up-DEGs and 1140 down-DEGs compared to the WT (Supplemental Figure S2A; Supplemental Data Set S1). The up- and down-DEGs were subject to Gene Ontology (GO) enrichment analysis using the GO Term Enrichment tool on TAIR (https://www.arabidopsis.org/tools/go_term_enrichment.jsp). Among up-DEGs for the *los2-5* mutant, GO terms related to immune responses such as "response to salicylic acid", "response to chitin" and "defense response to fungus" were highly enriched (Figure 3A). In particular, genes involved in response to SA were overrepresented (Figure 3A). Genes associated with "plant-type hypersensitive response" and "response to reactive oxygen species" were also enriched (Figure 3A). This was consistent with the H_2O_2 accumulation and cell death phenotypes observed in the *los2* mutants (Figure 2, D and E). In contrast, genes associated with plant growth and development, metabolism and response to abiotic stresses were overrepresented among down-DEGs of *los2-5* mutant (Figure 3B). GO terms associated with primary metabolism such as reductive pentose-phosphate cycle, gluconeogenesis, and fatty acid biosynthetic

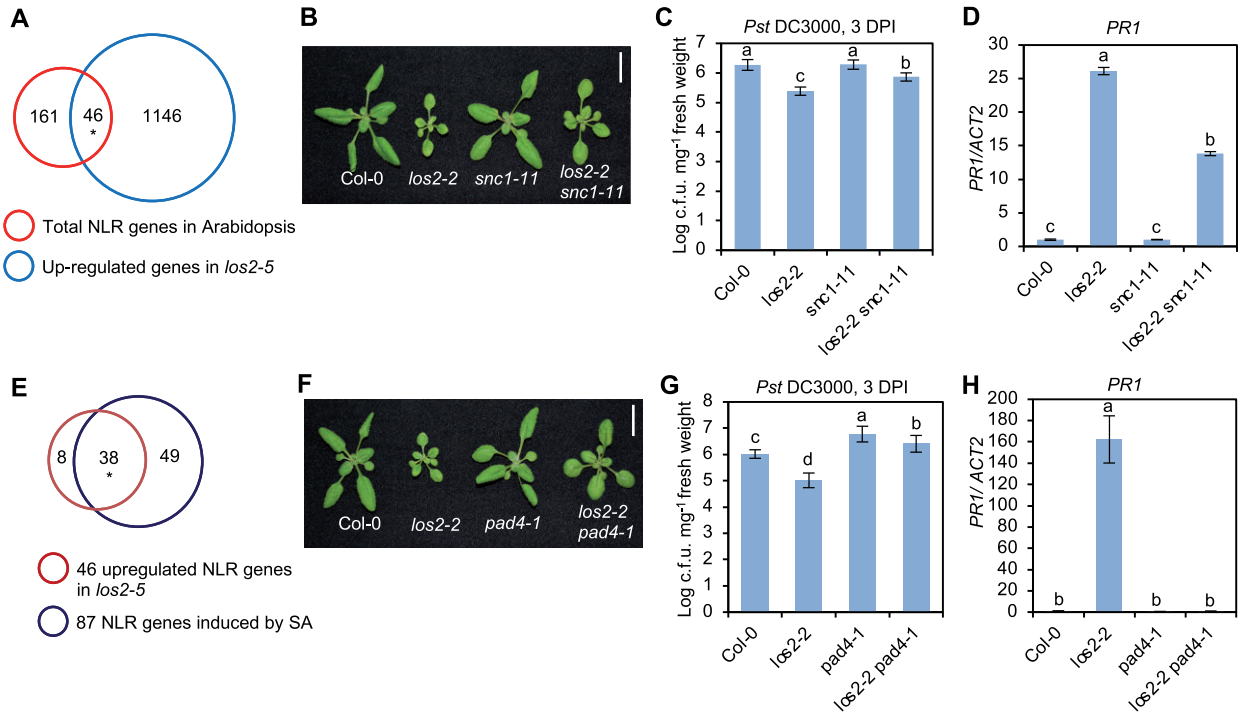

Figure 4 NLR genes and NLR/SA signaling contribute to *LOS2*-mediated immune responses. A, Venn diagram of 1192 upregulated genes in *los2-5* mutant and 207 total NLR genes in Arabidopsis. Asterisk indicates a significant difference tested by Fisher's exact test, $P < 3.158e{-}14$. B, Morphology and quantification of weight of Col-0, *los2-2*, *snc1-11* and *los2-2 snc1-11*. Scale bar = 1 cm. C and D, Growth of bacterial pathogen *Pst* DC3000 (C) and analysis of *PR1* gene expression (D) in Col-0, *los2-2*, *snc1-11* and *los2-2 snc1-11*. E, Venn diagram of 46 upregulated NLR genes in *los2-5* mutant and 87 SA-induced NLR genes in Arabidopsis. Asterisk indicates a significant difference tested by Fisher's exact test, $P < 6.917e{-}90$. F, Morphology of Col-0, *los2-2*, *pad4-1* and *los2-2 pad4-1*. Scale bar = 1 cm. G and H, Growth of bacterial pathogen *Pst* DC3000 (G) and analysis of *PR1* gene expression (H) in Col-0, *los2-2*, *pad4-1* and *los2-2 pad4-1*. Six biological replicates were performed for (C) and (G). Three biological replicates were performed for (D) and (H). Error bars represent SD. Different letters indicate significant difference tested by one-way ANOVA/Duncan's multiple range test via R 3.6.3 with "agricolae" package, $P < 0.05$. DPI, days post-inoculation.

process were enriched in down-DEGs of the mutant versus the WT (Figure 3B). Since LOS2 is a glycolytic enzyme, a defect in glycolysis in the *los2-5* mutant is expected to affect plant metabolism. Chlorophyll biosynthetic process was overrepresented in DEGs (Figure 3B), which was consistent with the observation that the *los2* mutants had less chlorophyll content compared to WT (Supplemental Figure S1F). Additionally, genes involved in cold acclimation were enriched among downregulated genes in *los2-5* mutant (Figure 3B). An altered expression of cold-response genes had also been reported for the *los2-1* mutant (Lee et al., 2002). These results support that *LOS2* is a negative regulator of plant immunity while being a positive regulator of plant growth and development.

The autoimmunity in *los2-2* mutant is dependent on the NLR/SA pathway and reduces plant growth

To assess the involvement of SA in the autoimmunity in the *los2* mutant as revealed by the RNA-seq data, we first quantified the SA level in the *los2* mutant. The *los2-2* mutant accumulated about 40% more free SA than the WT in the absence of pathogen infection (Figure 3C). To assess the role of SA increase in autoimmunity, we introduced into *los2-2* mutant the *NahG* gene which encodes a salicylate hydroxylase to degrade SA. The *NahG* transgene largely suppressed the growth defect of *los2-2*, and the *los2 nahG* plant had significantly larger rosette size compared to the *los2-2* mutant (Figure 3D; Supplemental Figure S2B). The *NahG* transgene also reduced the elevated immune responses in the *los2-2* mutant, including enhanced resistance to *Pst* DC3000 and increased *PR1* expression (Figure 3, E and F). This indicates that SA increase is responsible for autoimmunity and partially accounts for growth defects of *los2*.

Since *los2-5* was identified as a suppressor of *bon1 mos1* mutant where upregulation of the NLR gene *SNC1* is the key for autoimmunity, we asked whether NLR genes played a role in *LOS2*-repressed immune responses. In *Arabidopsis thaliana* Col-0 accession, 207 NLR or NLR-like genes (hereafter, *NLR* genes) are identified (Meyers et al., 2003). RNA-seq data revealed that 46 *NLR* genes were upregulated in *los2-5* mutant and no *NLR* genes were downregulated in *los2-5* mutant (Figure 4A). The contribution of the *SNC1* gene to the elevated immune responses in *los2* mutant was examined by introducing the loss of *SNC1* mutation *snc1-11* into *los2-2* (Figure 4B). The *los2-2 snc1-11* double mutant had reduced disease resistance and *PR1* gene expression compared

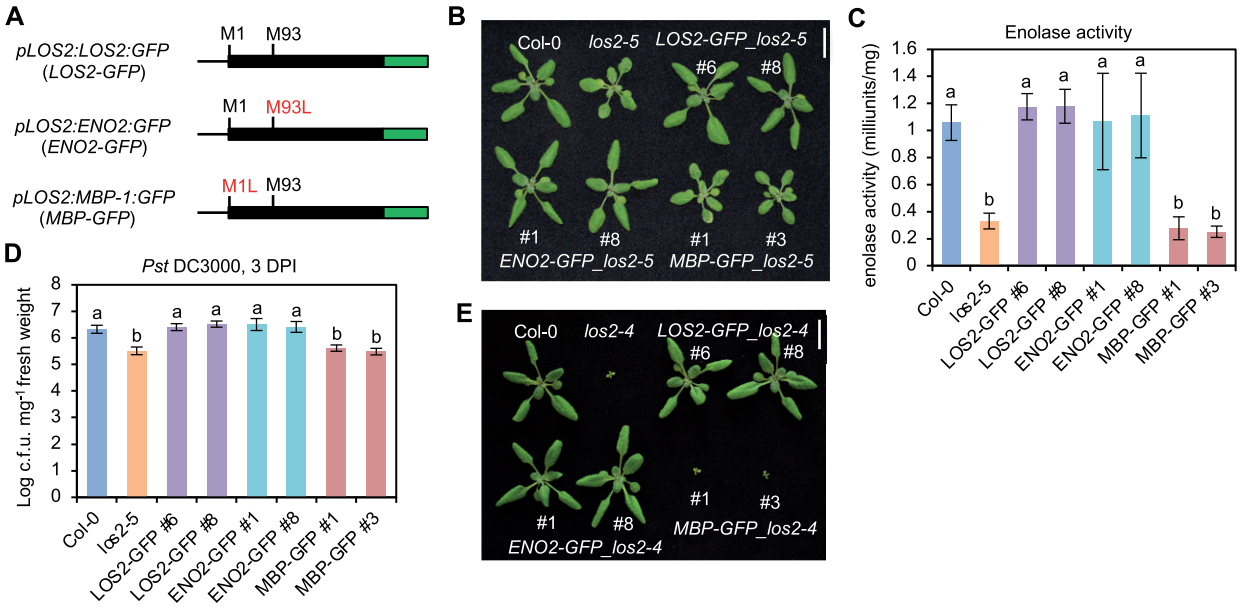

Figure 5 ENO2, but not MBP-1, contributes to plant growth and immunity regulation. A, Simplified gene structures of fusion proteins LOS2-GFP and two mutated forms ENO2-GFP and MBP-GFP. Genomic DNA was used for fusing with GFP. B–D, Morphology (B), enolase activity (C), and growth of bacterial pathogen *Pst* DC3000 (D) of Col-0, *los2-5* and complementation lines of LOS2-GFP (#6 and #8), ENO2-GFP (#1 and #8) and MBP-GFP (#1 and #3) in *los2-5* background. E, Morphology of Col-0, *los2-4* and complementation lines of LOS2-GFP (#6 and #8), ENO2-GFP (#1 and #8), and MBP-GFP (#1 and #3) in *los2-4* background. Four and six biological replicates were performed for (C) and (D), respectively. Error bars represent SD. Different letters indicate significant difference tested by one-way ANOVA/Duncan's multiple range test via R 3.6.3 with "agricolae" package, $P < 0.05$. Scale bar = 1 cm for (B) and (E). ; L, leucine; M, methionine.

to the *los2-2* mutant (Figure 4, C and D). These results suggest that *SNC1*, and perhaps other *NLR* genes, play a critical role in the activated immune responses in the *los2* mutants.

SA and NLR signaling are intertwined as NLR activation can induce SA and many *NLR* genes are induced by SA (Yang et al., 2021). Among the 46 *NLR* genes upregulated in *los2* mutant, 38 *NLR* genes can be induced by SA (Figure 4E). This suggested an amplification signaling loop from NLR to SA and to NLR in the *los2* mutant. To test the involvement of NLR/SA amplification in autoimmunity of *los2*, we introduced in *los2-2* a loss-of-function mutation of *PAD4*, a critical component in SA- and NLR-mediated immune signaling (Figure 4F). The *pad4-1* mutant reduced the accumulation of SA in *los2-2* to WT level (Figure 3C), indicating that the over-accumulation of SA in *los2-2* mutant was dependent on functional *PAD4*. Additionally, the enhanced resistance to *Pst* DC3000 and increased *PR1* expression in the *los2-2* mutant were largely decreased by the *pad4-1* mutation (Figure 4, G and H). This indicates that the *los2* autoimmunity is dependent on the function of *PAD4*.

Because autoimmunity leads to growth defects, we examined its contribution to the defects of growth and development observed in the *los2* mutants. We used *pad4* and *snc1* mutation to block or reduce autoimmunity in *los2-2*. The double mutant *los2-2 pad4-1* displayed similar flowering time and chlorophyll content to the *los2-2* mutant (Supplemental Figure 3, A and B). In contrast, both the double mutants *los2-2 snc1-11* and *los2-2 pad4-1* had a larger rosette size as compared to the *los2-2* mutant but were still smaller compared to the WT (Figure 4, B and F; Supplemental Figure S3, C and D). This indicates that the growth defects of the *los2* mutants are not entirely due to a deficiency in primary metabolism but rather due to the activated defense responses to a large extent.

The enolase form is important for the *LOS2* function in growth and immunity regulation

The *LOS2* gene was postulated to encode two isoforms, enolase and MBP-1, via different translation initiation sites (Kang et al., 2013), and its function in abiotic stress response was attributed to the transcriptional repressor MBP-1 (Kang et al., 2013; Liu et al., 2017). We tested the contribution of these two alternatively translated proteins to the different roles of the *LOS2* gene. For simplicity, we named the long protein form starting from the first methionine as ENO2 (enolase) and the short protein form starting from the second methionine residue +93 as MBP. The *LOS2* genomic fragment was in vitro mutagenized so that only one protein form was expected to be produced from the *LOS2* gene, and the proteins were tagged by GFP at their C-termini to aid protein detection (Figure 5A). The Met93 mutation to Leu (M93L) was expected to produce only the long form ENO2 (*pLOS2:ENO2:GFP* or *ENO2-GFP*), and Met1 mutation to Leu (M1L) was expected to produce only the short form MBP (*pLOS2:MBP:GFP* or *MBP-GFP*) (Figure 5A). These constructs were transformed into the *los2-5* mutant background, which had no defects in seed setting. A similarly

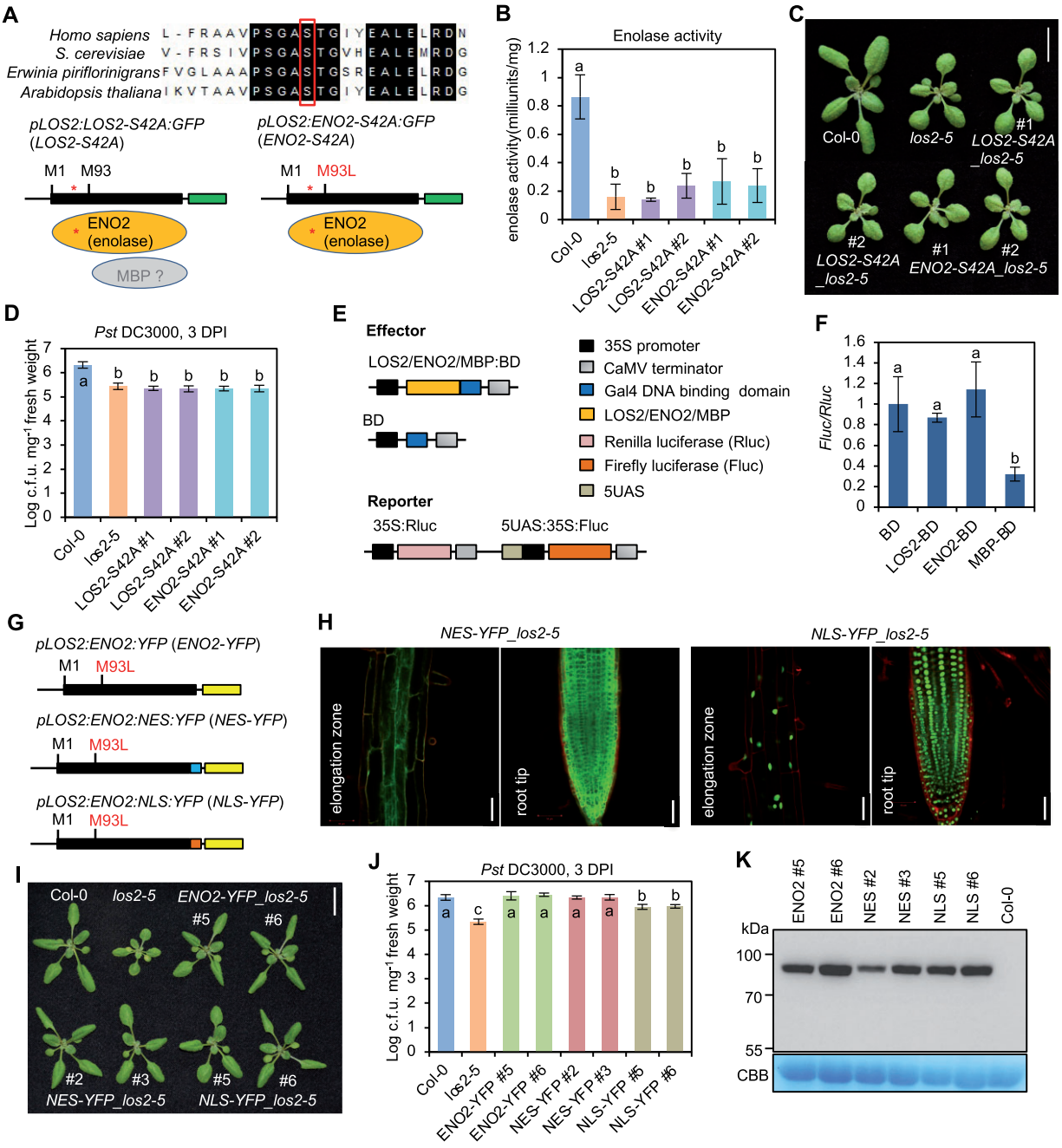

Figure 6 The enzymatic activity of ENO2 contributes to plant growth and immunity regulation. A, Sequence alignment of enolases from human, yeast, bacterium, and Arabidopsis. The partial alignment result is shown. The red box and star indicate the serine at position 42 in Arabidopsis which was mutated into Alanine (S42A). B–D, Enolase activity (B), morphology (C), and growth of bacterial pathogen *Pst* DC3000 (D) in Col-0, *los2-5* and two representative lines of *pLOS2:LOS2-S42A:GFP* and *pLOS2:ENO2-S42A:GFP* in *los2-5* background. E, Schematics of constructs used for the dual-luciferase reporter assay. F, Firefly luciferase expression level after normalized to renilla luciferase expression. The expression of BD was set to 1. G, Simplified gene structure for fusion proteins ENO2-YFP, NES-GFP, and NLS-GFP. H, Confocal imaging of fusion proteins in Arabidopsis root treated with propidium iodide. Scale bar = 50 μm. I, Morphology of Col-0, *los2-5* and complementation lines of ENO2-YFP (#5 and #6), NES-YFP (#2 and #3) and NLS-YFP (#5 and #6) in *los2-5* background. J, Growth of bacterial pathogen *Pst* DC3000 in Col-0, *los2-5*, ENO2-YFP (#5 and #6), NES-YFP (#2 and #3) and NLS-YFP (#5 and #6) in *los2-5* background. K, Immunoblot detecting the fusion proteins by anti-GFP antibody in complementation lines of ENO2-YFP (#5 and #6), NES-YFP (#2 and #3), and NLS-YFP (#5 and #6) in *los2-5* background. Col-0 was used as a negative control. Four and three biological replicates were performed for (B) and (F), respectively. Six biological replicates were performed for (D) and (J). Error bars represent SD. Different letters indicate significant difference tested by one-way ANOVA/Duncan's multiple range test via R 3.6.3 with "agricolae" package, $P < 0.05$. Scale bar in (C) and (I) is 1 cm. CBB, Coomassie brilliant blue.

constructed WT *LOS2* gene, *pLOS2:LOS2:GFP* (*LOS2-GFP*), was also transformed into the *los2-5* mutant as a control. Of the 13 independent transgenic lines harboring *LOS2-GFP*, all had a WT phenotype, indicating that the GFP tag did not compromise the LOS2 activity in rescuing the *los2-5* defects. Analysis of two representative transgenic lines (#6 and #8) harboring *LOS2-GFP* in *los2-5* revealed WT enolase activity, biomass and WT level of disease resistance to *Pst* DC3000 in these lines (Figure 5, B–D; Supplemental Figure S4A). Interestingly, of the 27 transgenic lines containing the ENO2 form, all exhibited a WT growth phenotype, similarly to the LOS2 form. Two representative *ENO2-GFP* lines in *los2-5* (#1 and #8) analyzed also exhibited WT phenotypes in enolase activity, biomass, and disease resistance (Figure 5, B–D; Supplemental Figure S4A). In contrast, *MBP-GFP* did not rescue growth defects of the *los2-5* mutant in any of the 12 transgenic lines analyzed. Two representative *MBP-GFP* transgenic plants (#1 and #3) analyzed were similar to the *los2-5* mutant in enolase activity, biomass, and resistance to *Pst* DC3000 (Figure 5, B–D; Supplemental Figure S4A). Together with the full rescue of *los2-5* by ENO2, this indicates that a lack of MBP production does not compromise the *LOS2* function in growth or immunity.

Because *los2-5* is a weak allele, it remained possible that a minor contribution from MBP was not measurable in this background but could be seen in the stronger allele *los2-4* background. As the *los2-4* mutant was too weak to be transformed, we introgressed the transgenes of *LOS2-GFP*, *ENO2-GFP*, and *MBP-GFP* from four independent lines in the weak allele *los2-5* background to the strong knock-down mutant *los2-4*. Similar to the observations in *los2-5*, *LOS2-GFP*, and *ENO2-GFP* both completely rescued the *los2-4* mutant defects while *MBP-GFP* did not (Figure 5E; Supplemental Figure S4B). These analyses further indicate that the ENO2 form alone but not MBP is sufficient to account for the function of *LOS2* in growth and immunity regulation.

The enzymatic activity but not transcriptional activity is critical for *LOS2* function in growth and immunity regulation

Since the ENO2 form is sufficient for the role of *LOS2* in growth and immunity regulation, we tested if the enolase activity of *LOS2* gene was critical for the regulation. To this end, we generated mutated forms of LOS2 and ENO2 in which serine at position 42 (S42) was mutated to alanine to abolish enolase activity (Figure 6A). The S42 residue in Arabidopsis is highly conserved among enolases in eukaryotes and prokaryotes (Figure 6A), and its corresponding S40 residue is critical for magnesium binding in human and is essential for enolase activity in yeast (Kang et al., 2008; https://www.uniprot.org/uniprot/P00924). Two constructs *pLOS2:LOS2-S42A:GFP* (*LOS2-S42A*) and *pLOS2:ENO2-S42A:GFP* (*ENO2-S42A*) containing the S42A mutation in *LOS2* and *ENO2*, respectively, were transformed into the *los2-5* background. Two representative transgenic lines for each construct were selected based on the comparable expression levels of fusion proteins (Supplemental Figure S5). The S42A mutation indeed eliminated the enolase activity of LOS2 and ENO2 as neither the *LOS2-S42A* nor the *ENO2-S42A* transgene restored the enolase activity in the *los2-5* mutant (Figure 6B). Importantly, these catalytic dead transgenes, unlike their WT counterparts, could not complement the growth or immunity defects of the *los2-5* mutant (Figure 6, C and D; Supplemental Figure S6A). These results indicate the importance of enolase activity of LOS2 in plant growth and immunity regulation.

Because the C-terminus of ENO2 protein has the same amino acid sequences as the postulated MBP protein, we asked whether the ENO2 protein could execute the transcriptional repressor activity as MBP-1 protein in mammalian cells. We utilized a dual-luciferase reporter assay in Arabidopsis protoplasts to examine the repressor activity (Figure 6E). Effector proteins including LOS2, ENO2, and MBP were fused to Gal4 DNA binding domain (BD), respectively. Each effector construct was co-transformed with a reporter construct into protoplasts, and the expression of firefly luciferase was used as an indicator of the transcription repressor activity of the effector. Protoplasts co-transformed either LOS2-BD or ENO2-BD with the reporter exhibited a similar luciferase activity as compared to that of the empty control BD (Figure 6F). In contrast, protoplasts harboring MBP-BD and reporter showed a significantly decreased expression of luciferase as compared to the control BD (Figure 6F). These data suggest that ENO2 may not have a transcriptional repressor activity.

To further examine the potential function of ENO2 as a transcriptional repressor, we tested the function of a nucleus-excluded ENO2 form in plants. The YFP-tagged ENO2 protein was fused with a nuclear export signal (NES) and transformed into the *los2-5* mutant background (Figure 6G). While the ENO2-YFP protein was found in both nucleus and cytosol (Kang et al., 2013), the ENO2-NES-YFP was found solely in cytosol (Figure 6H). As expected, the *ENO2-YFP* transgene completely rescued the *los2-5* growth and immunity defects (Figure 6, I and J; Supplemental Figure S6B). Interestingly, *ENO2-NES* also fully complement *los2* mutant phenotypes in growth and immunity (Figure 6, I and J; Supplemental Figure S6B). This indicates that ENO2 in cytosol is sufficient to carry out all functions of *LOS2* in plant growth and immunity regulation, arguing against an involvement of transcriptional repressor activity in this regulation. In addition, we generated a nucleus localized ENO2-YFP by fusing it to a nuclear localization signal (NLS) and transformed it into *los2-5*. Microscopy on transgenic plants revealed that the florescent signal from the ENO2-NLS-YFP protein was accumulated in the nucleus (Figure 6H). This ENO2-NLS-YFP form, unlike the ENO2-YFP or ENO2-NES-YFP, did not rescue the immunity defects of *los2-5*, but it did rescue its growth defect (Figure 6, I and J; Supplemental Figure S6B). We excluded the possibility that a lower protein expression of ENO2-NLS-YFP was responsible for the difference because immunoblot analysis showed that *ENO2-YFP* and *ENO2-NLS-YFP* had comparable protein levels

even with line #2 of *ENO2-NES-YFP* having the lowest protein expression (Figure 6K). This indicates that the ENO2-NES form has the same activity as ENO2 while ENO2-NLS has a lower activity than ENO2. Therefore, the cytosolic function of ENO2 can account for all activities of *LOS2*. The partial activity of ENO2-NLS might be due to its transient and small amount of cytosol accumulation.

Autoimmunity in the *los2* mutants induces accumulation of sugars and organic acids

We measured the amount of some core primary metabolites in the *los2* mutants to assess how the reduction of glycolysis enzyme affects primary metabolism and whether autoimmunity has an indirect effect on primary metabolism as it does to plant growth. Sucrose, glucose, galactose, fructose, maltose, malic acid, and citric acid were quantified in leaves of Col-0 WT, *los2-5*, and *los2-2* plants by gas chromatography-mass spectrometry (GC-MS) analysis. The *los2-5* mutant had a higher accumulation of all these metabolites compared to WT (Figure 7A). Likewise, the *los2-2* mutant accumulated more sucrose, glucose, malic acid, citric acid, and maltose (Figure 7A). The difference in fructose and galactose amount between the *los2-2* mutant and the WT could not be assessed due to the low amount of these sugars and large measurement variations (Figure 7A).

The amounts of sucrose, glucose, malic acid, and citric acid were measured in the *los2-2 pad4-1* mutant where autoimmunity was largely suppressed (Figure 4, F–H). Interestingly, the *pad4* mutation completely abolished the higher accumulation of sucrose and malic acid, and partially suppressed the higher accumulation of glucose and citric acid in *los2-2* mutant (Figure 7B). Additionally, the *pad4-1* single mutant had a reduced accumulation of these metabolites as compared to WT, and the *los2-2 pad4-1* mutant had a similar amount of sucrose and malic acid as the *pad4* mutant (Figure 7B). The change of primary metabolite amount was not simply a result from the change of plant size, because the *los2-2* and *los2-5* mutants, with one-fold difference in fresh weight (Figure 2A), had a similar amount change of most of the metabolites measured (Figure 7A). These results suggest that the increased accumulation of primary metabolites in the *los2* mutants is largely due to activated immune responses. Interestingly, the *pad4* mutant had a slightly lower accumulation of primary metabolites, further suggesting a promotion of some primary metabolites by an increase of defense responses.

Autoimmunity in the *los2* mutants perturbs glycolysis

We further quantified the relative amount of six major glycolytic metabolites in Col-0 WT, *los2-2*, and *los2-2 pad4-1* plants by high performance liquid chromatography (HPLC)-mass spectrometry (MS) analysis (Figure 7, C and D). These included β-D-fructose 6-phosphate (F6P), β-D-fructose 1,6-bisphosphate (FBP), D-glyceraldehyde 3-phosphate (GAP), 3-phospho-D-glycerate (3-PG), 2-PG, and PEP. Because 2-PG and 3-PG are structural isomers having the same monoisotopic mass and indistinguishable in the HPLC-MS analysis, the total relative amount of these two metabolites in each genotype was displayed as 2/3-PG. F6P and FBP accumulated to a similar level in WT and *los2-2*, but GAP, 2/3-PG, and PEP accumulated to a lower level in *los2-2* than in the WT (Figure 7C). The reduced GAP in the *los2-2* mutant was due to autoimmunity since the *pad4-1* mutation elevated the GAP level in *los2-2* mutant to the WT level (Figure 7C). By contrast, *pad4* mutation did not alter the reduced amount of 2/3-PG and PEP, the substrate and product of enolase, in *los2-2* compared to the WT (Figure 7, C and D). These results indicate that the reduction of LOS2 activity perturbs glycolysis and the resulting autoimmunity further affects primary metabolites.

The MBP protein is detected only when overexpressed under a non-native gene context

Since the putative MBP form when made from the native content is dispensable for the *LOS2* function, we examined the existence of MBP in Arabidopsis using above-mentioned transgenic lines expressing the genes under the native promoter of *LOS2*. All transgenic plants of *LOS2-GFP*, *ENO2-GFP*, and *MBP-GFP* in *los2-5* had comparable *LOS2* transcript levels (Figure 8A), indicating low transgene expression was not the reason for phenotypic differences observed in *ENO2-GFP* and *MBP-GFP* transgenic plants. Confocal microscopy on roots of transgenic plants revealed that LOS2-GFP was localized to both nucleus and cytoplasm in transgenic plants as previously reported (Lee et al., 2002; Kang et al., 2013; Figure 8B). ENO2-GFP had the same dual localization pattern as LOS2-GFP in transgenic plants (Figure 8B). However, GFP signal was not detectable in the *MBP-GFP* transgenic plants (Figure 8B). We further examined the accumulation of fusion proteins in two representative transgenic plants for each transgene by immunoblotting. While ENO2-GFP protein was detected at the expected size in the *ENO2-GFP* plants, no MBP-GFP protein was detected in the *MBP-GFP* plants by anti-GFP antibody (Figure 8C). Only one protein signal at the ENO2-GFP size could be detected from the *LOS2-GFP* transgenic plants and no MBP-GFP signal, which is expected to be 10 kDa smaller than the ENO2-GFP, could be detected (Figure 8C). Serial dilution of the protein extracts revealed that the MBP form, if produced, would be at least 250-fold less than the ENO2 form from the *LOS2-GFP* transgene (Figure 8D). Since MBP protein was reported to be subject to ubiquitin-dependent degradation (Kang et al., 2013), we examined the presence of MBP proteins in *LOS2-GFP* transgenic lines after MG132 (a ubiquitin-dependent proteasome inhibitor) treatment by immunoblotting. All four independent *LOS2-GFP* transgenic lines examined produced only the ENO2 form with or without MG132 treatment, and no MBP protein could be detected even with MG132 treatment (Figure 8E). These results indicate the absence or very low abundance of an

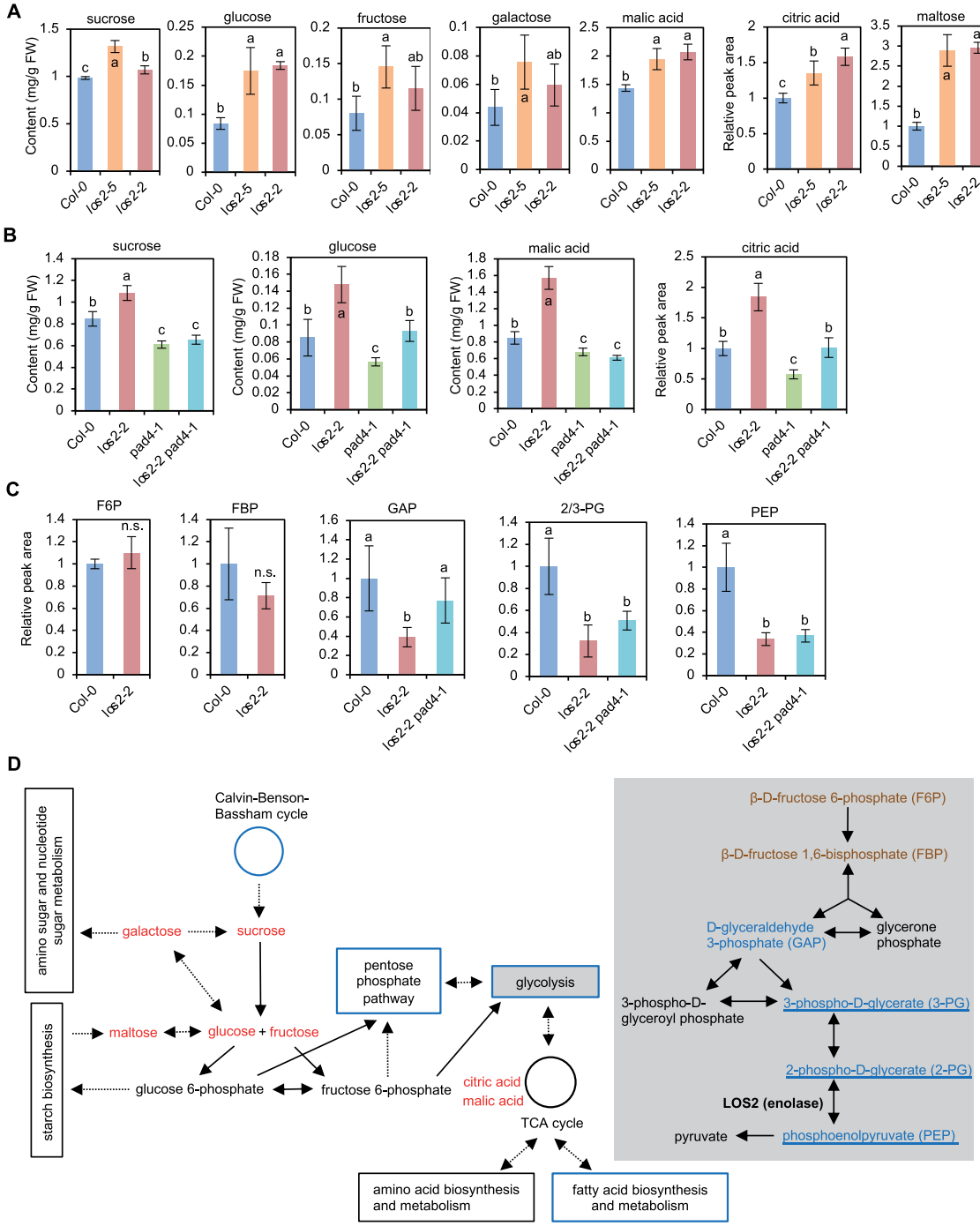

Figure 7 The *los2* mutants have altered primary metabolite homeostasis. A, Absolute content of sucrose, glucose, fructose, galactose, and malic acid as well as relative peak area of citric acid and maltose in Col-0, *los2-5* and *los2-2* measured by GC–MS. The relative amount of citric acid and maltose was calculated in respect to the amount of internal control in the samples and values were normalized to Col-0. B, Absolute content of sucrose, glucose, and malic acid as well as the relative peak area of citric acid in Col-0, *los2-2*, *pad4-1* and *los2-2 pad4-1* measured by GC–MS. The relative amount of citric acid was calculated in respect to the amount of internal control in the samples and values were normalized to Col-0. C, Relative peak area of glycolytic metabolites in Col-0, *los2-2* and *los2-2 pad4-1* measured by HPLC. The value of Col-0 WT was set as "1" and the value of others was normalized to the value of Col-0. D, Simplified schematic presentation of the connection between glycolysis and other major primary metabolic pathways. Glycolysis pathway was colored light gray in the background. Solid arrows indicate one single biochemical reaction while dashed arrows represent multiple biochemical reactions. Metabolites increased or decreased in the *los2-2* mutant as compared to WT were colored red or blue, respectively; metabolites having comparable amount in the *los2-2* mutant and WT were colored mocha. Pathways that were enriched in the GO term analysis of downregulated genes in *los2-5* mutant (Figure 3B) were boxed or cycled with blue. Metabolites that were not dependent on functional PAD4 were underlined. Five biological replicates were performed for (A), (B), and (C). Error bars represent SD. Different letters indicate significant difference tested by one-way ANOVA/Duncan's multiple range test via R 3.6.3 with "agricolae" package, $P < 0.05$. "n.s." indicates no significant difference tested by Student *t* test, $P < 0.05$. FW, fresh weight. TCA cycle: The tricarboxylic acid cycle.

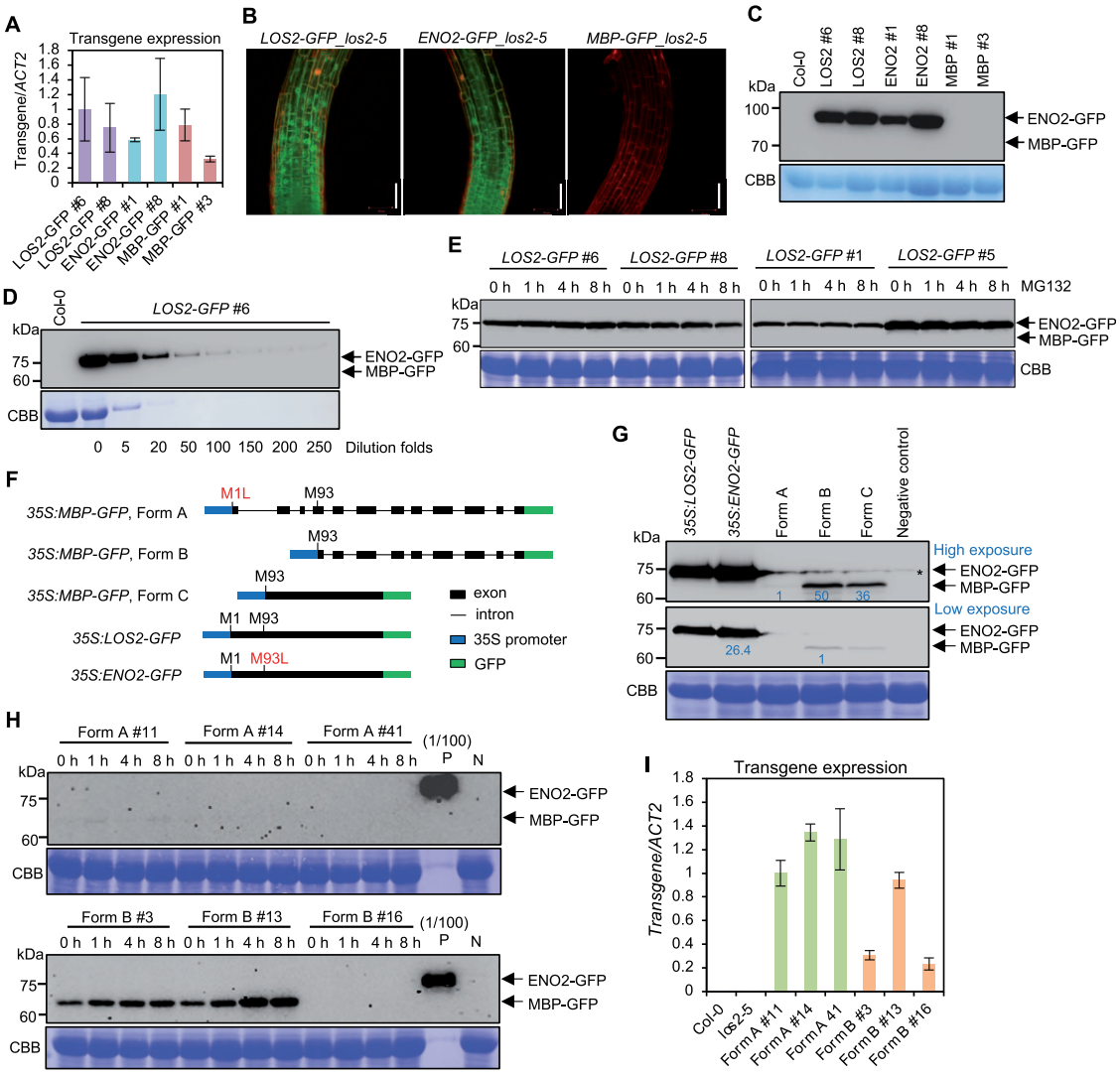

Figure 8 Endogenous MBP cannot be detected in Arabidopsis under the native *LOS2* gene context. A, Analysis of transgene expression in complementation lines of LOS2-GFP (#6 and #8), ENO2-GFP (#1 and #8), and MBP-GFP (#1 and #3). The expression of LOS2-GFP #6 was set to 1. B, Confocal microscopy showing the expression pattern of LOS2-GFP, ENO2-GFP, and MBP-GFP in Arabidopsis root treated with propidium iodide. Scale bar = 50 μm. C, Immunoblot detecting the fusion protein by anti-GFP antibody in complementation lines of LOS2-GFP (#6 and #8), ENO2-GFP (#1 and #8), and MBP-GFP (#1 and #3) in *los2-5* background. Col-0 was used as a negative control. D, Immunoblot of LOS2-GFP #6 using anti-GFP antibody. The number under each band indicated the dilution folds of LOS2-GFP #6 total proteins. Col-0 was used as a negative control. E, Immunoblot detecting ENO2-GFP and MBP-GFP proteins by anti-GFP antibody in four independent lines of LOS2-GFP (#6, #8, #1, and #5) after 50-μM MG132 treatment for 1, 4, and 8 h. F, Simplified gene structures of fusion proteins LOS2-GFP, ENO2-GFP, and three forms of MBP-GFP all of which were driven by 35S promoter. CDS of LOS2 and ENO2 were fused with GFP to form LOS2-GFP and ENO2-GFP. LOS2 genomic DNA with the first translation initiation site mutated (M1L) was fused with GFP to generate MBP-GFP (Form A) while LOS2 genomic DNA lacking the N-terminal sequence was fused with GFP for MBP-GFP (Form B). MBP-GFP (Form C) contains MBP CDS fused with GFP. G, Immunoblot detecting the fusion proteins expressed in *N. benthamiana* using anti-GFP antibody. Negative control was a sample without infiltration. Asterisk indicates a non-specific band detected in the samples. Protein levels were quantified by ImageJ. For the upper, proteins from Forms B and C were normalized to proteins from Form A; for the lower, ENO2-GFP was normalized to proteins from Form B. Blue letters indicated the fold changes. H, Immunoblot of MBP proteins from transgenic plants of Form A (#11, #14, and #41) and Form B (#3, #13, and #16) treated with 50 μM MG132 for 1, 4, and 8 h. Each form had two representative lines in which MBP could be detected (#11 and #14 from Form A; #3 and #13 from Form B) and one representative line in which MBP could not be detected (#41 from Form A and #16 from Form B) under normal conditions. "(1/100) P," positive control sample from *pLOS2:LOS2:GFP* #6 diluted 100 times. The same amounts of protein from positive control and negative control samples were loaded for the upper and lower blots. I, Transgene expression of three independent lines of *35S:MBP* (Form A)*:GFP* and *35S:MBP* (Form B)*:GFP*. The expression of Form A #11 was set to "1." Three biological replicates were performed for (A) and (I), and error bars represented SD. For transgene expression analysis, the forward primer targeted *LOS2* sequences and the reverse primer targeted *GFP* sequences. This same primer pair was able to amplify each of the three transgenes. Arrows in (C–E) and (G and H) indicate the expected size of ENO2(enolase)-GFP and MBP-GFP fusion proteins. CBB, Coomassie brilliant blue; L, leucine; M, methionine; N, negative control sample from Col-0.

endogenous MBP protein in plants under the growth condition investigated.

To increase the chance of detection of MBP, we overexpressed the *LOS2* gene transiently in *Nicotiana benthamiana*. The *LOS2* coding sequence (CDS) was fused with GFP at the C-terminus and driven by the 35S promoter to generate the construct *35S:LOS2-GFP* (Figure 8F). As a control, *ENO2* CDS fused with GFP was similarly expressed under the 35S promoter to generate the construct *35S:ENO2-GFP*. Both the *35S:LOS2-GFP* and *35S:ENO2-GFP* constructs produced ENO2-GFP at the expected size (Figure 8G; Supplemental Figure S7). However, no protein at the MBP-GFP size could be detected from *35S:LOS2-GFP* (Figure 8G; Supplemental Figure S7). These results indicate that MBP protein could not be detected even when under the CDS of *LOS2* was expressed in *N. benthamiana*.

A previous study detected MBP protein when sequence encoding only the MBP part of *LOS2* gene was expressed under the control of the 35S promoter (Kang et al., 2013; Liu et al., 2017). We therefore examined whether the detection of MBP was due to the deletion of the leader sequences 5′ to the MBP CDS in the earlier overexpression construct. We generated three *LOS2* forms varying in the leader sequence but were all expected to express the MBP protein but not ENO2 (Figure 8F). Form A was a *LOS2* genomic DNA fragment starting from the first translation initiation site but with this Met codon mutated to Leu. Form B was a *LOS2* genomic DNA fragment starting from the putative second translation initiation site. Form C started from the putative second translation site similar to Form B, but having CDS instead of genomic DNA of *LOS2*. All three variants were fused with GFP at the C-terminus and transiently expressed in *N. benthamiana* under the control of the 35S promoter (Figure 8, F and G). MBP-GFP could be detected from Form B and Form C, but at a much lower level ($<4\%$) compared to ENO2-GFP that was expressed in *N. benthamiana* as well (Figure 8G). Intriguingly, MBP-GFP could be detected only under a very long exposure from Form A variant, which best mimicked the endogenous genomic context (Figure 8G). The expression level of MBP protein from Form A was about 1/50 and 1/36 of that from Forms B and C, respectively (Figure 8G). These results indicate that the MBP protein could be produced in small amount when the sequence coding for MBP only was directly overexpressed and that M93 is not an effective alternative translation start site or not a site at all under the native context of the *LOS2* gene.

This observation from transient expression in *N. benthamiana* was also seen in transgenic Arabidopsis plants expressing the Form A and Form B variants respectively. Only 2 out of 24 Form A transgenic lines had detectable MBP expression, while 7 out of 21 Form B transgenic lines had detectable MBP protein. In addition, expressions in Form A lines were much lower than that in Form B lines (Figure 8H), while the transgene transcripts were expressed at a comparable level (Figure 8I). Quantification of the immunoblot signals revealed that the MBP protein from Form B overexpression was at least 100-fold lower in amount than the ENO2 expressed under the control of the *LOS2* native promoter (Figure 8H). We further treated transgenic plants with MG132 as it was reported to stabilize MBP (Kang et al., 2013). A moderate increase of MBP protein was observed with MG132 treatment, but MBP remained undetectable in lines where it was not detected without treatment (Figure 8H). Taken together, these results show that the production of MBP protein cannot be observed under the endogenous genomic context in the conditions tested and MBP can be produced at a very low amount when the sequence coding for MBP only (without its 5′-flanking sequences) is expressed under the control of 35S promoter.

MBP protein does not contribute to the *LOS2* function in development or expression of cold-response genes

We further asked if the enolase function rather than the putative MBP is responsible for the role of *LOS2* in plant development similarly to its role in immunity. *LOS2*, *ENO2*, and *MBP* were each expressed under the control of the *LOS2* native promoter, via constructs *pLOS2:LOS2:GFP* (*LOS2-GFP*), *pLOS2:ENO2:YFP* (*ENO2-YFP*), and *pLOS2:MBP:GFP* (*MBP-GFP*), and were introduced in the *los2-2* mutant which displayed a more drastic developmental defects compared to *los2-5* (Supplemental Figure S1, D–F). Similar to findings with these forms expressed under the *LOS2* native promoter (Figure 8, C–E), MBP-GFP could not be detected in the *LOS2-GFP* or *MBP-GFP* transgenic plants while ENO2 fusion protein was readily detected in *LOS2-GFP* and *ENO2-YFP* transgenic lines (Supplemental Figure S8A), despite a comparable RNA expression of *MBP-GFP* and *LOS2-GFP* transgene (Supplemental Figure S8B). Two representative transgenic lines from each transgene were analyzed for their growth, development, and immunity phenotypes. Transgenic lines of *LOS2-GFP* and *ENO2-YFP*, but not *MBP-GFP*, in *los2-2* mutant had WT fresh weight, chlorophyll content, flowering time, and silique length (Figure 9, A–E), indicating a full rescue of developmental defects. *LOS2-GFP* and *ENO2-YFP*, but not *MBP-GFP*, also rescued the disease resistance defect in *los2-2* (Figure 9F). These results demonstrate that enolase but not MBP contributes to the role of *LOS2* in plant growth and development.

The *LOS2* gene was found to contribute to freezing tolerance by modulating the expression of cold-response genes including *ZAT10* and *RD29A* in the Arabidopsis C24 ecotype (Lee et al., 2002). We investigated whether the enolase function of *LOS2* is responsible for its role in abiotic stress response. Expression of cold-responsive gene *RD29A* and its transcriptional repressor *ZAT10* was examined in the *los2-2* and *los2-5* mutants before and after 4°C treatment for 24 h. *ZAT10* had a higher expression in both mutants compared to the Col-0 WT before cold treatment (Figure 9G; Supplemental Figure S9A). It was significantly induced by cold treatment in all plants, but *ZAT10* had a higher

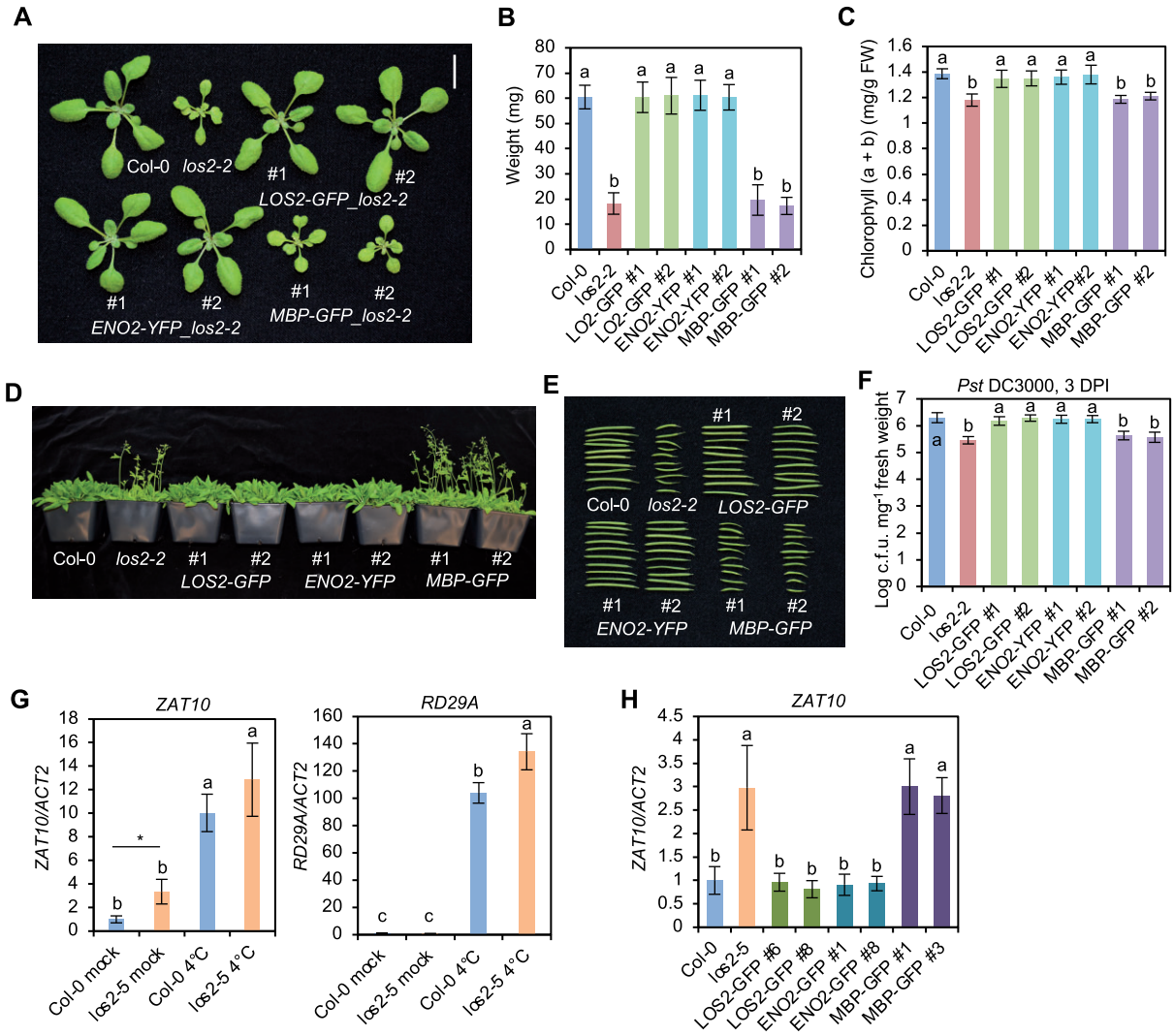

Figure 9 ENO2, but not MBP, rescues developmental defects and *ZAT10* gene expression in the *los2* mutant. A–F, Morphology (A), weight (B), chlorophyll amount (C), flowering (D), silique (E), and *Pst* DC3000 growth assay (F) of 2-week-old Col-0, *los2-2* and two representative transgenic lines of *pLOS2:LOS2:GFP* (*LOS2-GFP*), *pLOS2:ENO2:YFP* (ENO2-YFP) and *pLOS2:MBP:GFP* (MBP-GFP) in *los2-2* background. Scale bar in (A) is 1 cm and $N = 20$ for (B). G, Analysis of *ZAT10* and *RD29A* gene expression in Col-0 WT and *los2-5* mutant before (mock) and after 4°C treatment for 24 h (4°C). H, Analysis of *ZAT10* gene expression in Col-0 WT, *los2-5* mutant and complementation lines of LOS2-GFP (#6 and #8), ENO2-GFP (#1 and #8) and MBP-GFP (#1 and #3) in *los2-5* background under normal condition. Four and six biological replicates were performed for (C) and (F), respectively. Three biological replicates were performed for (G) and (H). Different letters indicate significant difference tested by one-way ANOVA/Duncan's multiple range test via R 3.6.3 with "agricolae" package, $P < 0.05$. Asterisk indicates a significant difference tested by Student's *t* test, $P < 0.05$. FW, fresh weight.

expression in *los2-2* but not in *los2-5* compared to the WT after cold treatment (Figure 9G; Supplemental Figure S9A). Surprisingly, although *RD29A* was highly induced by cold as expected, it had a higher expression in both the *los2-5* and *los2-2* mutants compared to the WT (Figure 9G; Supplemental Figure S9A). This is in contrast to the previous observation that *RD29A* had a lower expression in *los2-1* compared to the C24 WT under cold treatment (Lee et al., 2002). Similar to *RD29A*, two other cold-response genes *COR47* and *COR15A* did not have a reduced expression in the *los2-2* mutant compared to Col-0 WT after cold treatment (Supplemental Figure S9A). Therefore, the *los2-2* and *los2-5* mutants had higher expression of the repressor gene *ZAT10* (similarly to *los2-1* reported) but not lower expression of cold-response genes including *RD29A* after cold treatment (unlike the *los2-1* reported) compared to WT. These data do not support the early hypothesis that the increased expression of *ZAT10* by the loss of the transcriptional repressor function of *LOS2* leads to a reduced expression of cold-response genes. The reason for this expression difference of cold-response genes in *los2* mutants between this study and the previous study is not fully understood, and it might be due to the ecotype difference of *los2-1* (in C24) versus *los2-2* and *los2-5* (in Col-0) (Bechtold et al., 2018). Nevertheless, we examined the contribution of MBP to *LOS2* function in the expression regulation of cold-

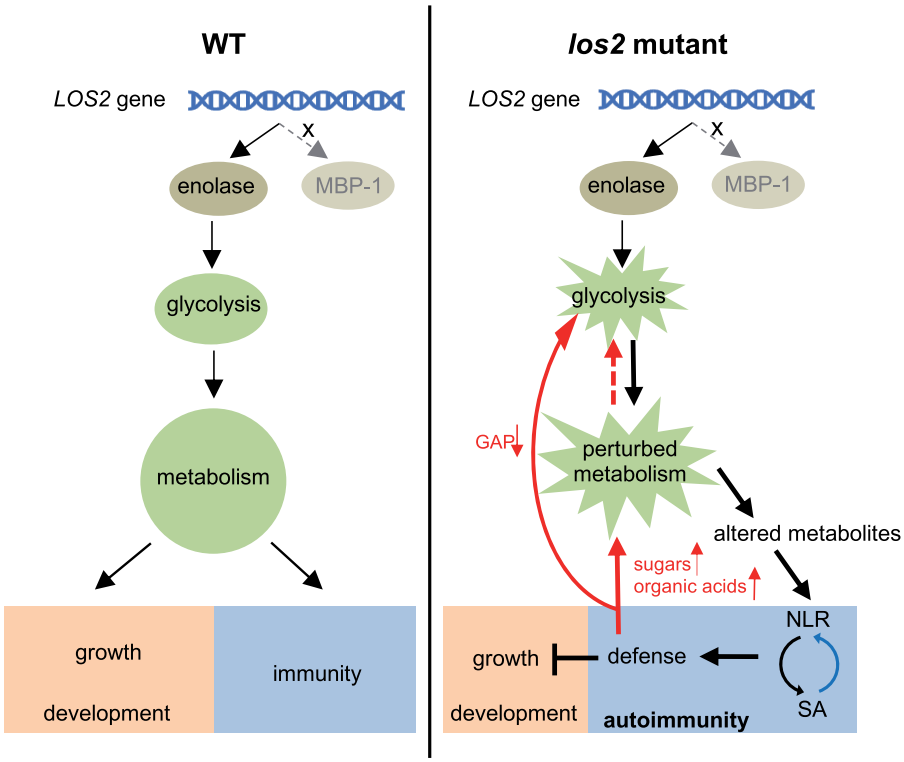

Figure 10 Working model for the role of *LOS2* in plant growth and immunity. The Arabidopsis *LOS2* gene encodes only a glycolytic enzyme enolase, but not the proposed MBP-1 protein. In WT plants, the homeostasis of glycolysis is critical for unperturbed metabolism and this is required for a balanced status of growth, development, and immunity. In the *los2* mutant, enolase activity is reduced, resulting in a perturbation of the glycolysis pathway and consequently of metabolism. The perturbed metabolism causes reduced growth and abnormal development. Importantly, the perturbed metabolism causes altered metabolites which might be sensed by NLR proteins or induce NLR transcription to trigger NLR activation. The activation of NLR proteins initiates downstream immune responses including the accumulation of SA which in turn induces NLR expression (blue arrow), resulting in a positive feedback loop to boost immunity. On one hand, defense responses repress plant growth, but not affect plant development. On the other hand, defense responses further disturb the perturbed metabolism (red arrows) by promoting the accumulation of sugars and organic acids or depleting of glycolytic metabolite GAP, leading to a second positive feedback loop for a robust immune response. Therefore, *LOS2* is critical for a balanced growth and defense status in plants by maintaining metabolism homeostasis.

response genes in the Col-0 accession. The *LOS2* and *ENO2* transgene totally reverted the higher than WT expression of *ZAT10* and *RD29A* in the *los2* mutants while *MBP* transgene had no effect on their expression in the *los2* mutants (Figure 9H; Supplemental Figure S9B). This result indicates that ENO2 but not MBP contributes to expression regulation of cold-response genes.

Discussion

Primary metabolism not only provides essential building blocks and energy for plant growth and development, but also is the source of secondary metabolites for diverse environmental responses including plant immune responses (Figure 10). This study uncovers an unexpected consequence of the perturbation of primary metabolism in activating defense responses rather than reducing immunity (Figure 10). The reduction of the glycolytic enolase function in *los2* mutant causes reduced growth, abnormal development, and alteration of cold-response gene expression. Importantly, it triggers an NLR/SA-mediated autoimmunity that is accompanied by high accumulation of SA. Autoimmunity contributes to the repression of plant growth by the *los2* mutation, but not the developmental defects in flowering time and silique development. Autoimmunity also influences metabolism by promoting the accumulation of sugars and organic acids and depletion of glycolytic metabolite GAP. Therefore, *LOS2* gene is critical for a balanced growth and defense status in plants by maintaining metabolism homeostasis (Figure 10).

This study reveals that *LOS2* affects plant immunity through its canonical function in glycolysis rather than an alternatively translated product MBP, which was postulated to be important for the *LOS2* function in abiotic stress tolerance. A mutation at the critical site for the enolase activity abolished the ability of enolase to rescue the *los2* mutant defects in growth and immunity (Figure 6, A–D). In addition, a mutated *LOS2* gene that cannot produce MBP is fully functional in Arabidopsis (Figure 5). These data indicate that LOS2 functions as the canonical glycolytic enolase and the alternatively translated MBP plays little if any role in Arabidopsis. This study further shows that the *LOS2* gene does not produce MBP or produces it at undetectable amounts under the conditions we analyzed in Arabidopsis (Figure 8, B–E). The MBP protein could be detected only at

low amount when the sequence coding for MBP only was driven by the 35S promoter (Figure 8, G and H; Supplemental Figure S7). The MBP production was reported in transgenic plants carrying a *LOS2-YFP* overexpression construct (Kang et al., 2013). As the transgenic line in the previous report was not available, we were unable to re-analyze that line together with transgenic lines generated in this study to determine if the growth conditions could be the reason for the discrepancy. It is possible that MBP is produced under specific conditions, considering that its putative translation start site M93 is conserved among homologs of *LOS2* in plants. Further studies using various stress treatment might reveal if and when MBP could be produced from the *LOS2* gene in plants. They may also reveal if this production might have some function in certain stress responses although it does not contribute to the role of *LOS2* in growth and immunity regulation.

It is important to make a distinction between the possible MBP function from a natively produced protein (from alternative translation from the *LOS2* locus) and the consequences of overexpression of a constructed MBP CDS free of its native gene context. Early studies of the role of MBP in abiotic stress responses and the function of MBP as a transcriptional repressor were mostly based on overexpression of the latter (Kang et al., 2013; Liu et al., 2017). It is possible that the MBP produced under the artificial condition could carry out a direct regulation on gene expression in abiotic responses, but it may not be the function of the endogenous *LOS2*. Intriguingly, overexpression of MBP in early studies induced a similar defect as the loss of *LOS2* function (Kang et al., 2013; Eremina et al., 2015). Although this was thought to be a feedback regulation from the repressor activity of MBP, it might result from gene silencing of the endogenous *LOS2* by *MBP* overexpression. Further studies could reveal whether MBP from overexpression has an effect on its own independently of the endogenous ENO2 from *LOS2*.

Data from this study do not support the hypothesis that the enolase protein has a second function as a transcriptional repressor. In addition, we show that this second function as a transcriptional repressor, if existing, is not critical for the enolase to regulate metabolism or impact growth and immunity. An earlier study found that the recombinant enolase protein can bind to the promoter sequences from the *ZAT10* gene in a gel shift assay (Lee et al., 2002). However, no binding of LOS2/ENO2 to DNA in vivo has been attempted, and no transcriptional repressor activity has been examined. We found that the full-length enolase (ENO2), unlike MBP, did not exhibit the transcriptional repressor activity in the reporter assay system (Figure 6F). In addition, the cytosol-localized enolase (ENO2-NES) was fully functional in growth and immunity regulation, supporting the importance of the enolase activity but not the transcriptional repressor activity of LOS2 (Figure 6, I and J). The partial functionality of the ENO2-NLS form might have resulted from small amount of cytoplasm-localized ENO2 protein from cytosol translation before being transported into nucleus. Further supporting the one-activity hypothesis is the full elimination of the LOS2/ENO2 function by the catalytic dead mutation of enolase (Figures 5 and 6, A–D). Therefore, LOS2 functions through its enolase activity in plants and its mutant defects result from perturbation of glycolysis which leads to altered gene expression in immune responses. Nevertheless, the possibility that LOS2/ENO2 might have transcriptional repressor activity under specific conditions or for other biological processes such as cold response is not excluded. However, future studies to explore this repressor possibility should fully consider the potential indirect impact from perturbed metabolism.

This study shows that growth defects of the *los2* mutants are not entirely due to the limit in primary metabolism but rather partially due to the activated defense responses. The dwarfism of the *los2-2* mutant was largely rescued when the SA-mediated immune signaling was blocked either by a loss of *PAD4* function or the *NahG* transgene (Figures 3, C–F and 4, F–H; Supplemental Figures S2B and S3D) while early flowering and reduced chlorophyll content of the *los2-2* mutant were not dependent on *PAD4* (Supplemental Figure 3, A and B). This implies that the *LOS2* gene has diverse roles, either directly through its glycolysis function or indirectly through its effect on immune activation.

This study raises questions on the function of *LOS2* in cold tolerance and perhaps other abiotic stress tolerance. The effect of the loss of *LOS2* function on cold response in the Col-0 accession is different from what was reported in the C24 accession. Although the cold-response repressor gene *ZAT10* (postulated as a target gene of the LOS2 transcriptional repressor) had higher expression in the *los2* mutants compared to WT, the cold-response marker gene *RD29A* (that is repressed by ZAT10) did not have a lower expression in the Col-0 *los2* mutants in contrast to the C24 *los2-1* mutant (Figure 9G; Supplemental Figure S9A). This suggests that the Col-0 *los2* mutants might not have a similar cold tolerance defect as the C24 *los2-1* mutant. It also raises the question of whether lower expression of *RD29A*, and thus compromised freezing tolerance, in the C24 *los2* mutant is through noncanonical transcriptional activity of LOS2 on the expression of genes like *ZAT10*. As low temperature responses and immune responses are highly connected (Saijo and Loo, 2020), it is important to re-evaluate the *LOS2* function in abiotic stress response to differentiate direct effects and indirect effects from metabolism perturbation or immune response activation. It is noted that C24 has unusual tolerance for multiple abiotic and biotic stresses without overt growth deficiency (Bechtold et al., 2018), suggesting a different wiring of growth, immune responses, and abiotic stress responses in C24 compared to the Col-0 accession. Molecular genetic dissection and comparison of the *LOS2* function in these accessions will further our understanding of the connection of primary metabolism and environmental responses.

The effect of the reduction of enolase activity on primary metabolism is complex. A decrease of the enolase product PEP was observed regardless of the immunity status (Figure 7C). A decrease was also seen for the total amount of 2-PG (substrate of enolase) and its direct precursor 3-PG in the *los2-2* mutant (Figure 7, C and D). This suggests that reducing enolase activity might lead to a decreased flux of glycolysis resulting in decreased substrate and product of enolase in the *los2* mutants. Strikingly, autoimmunity, but not reduction of enolase activity itself, resulted in an accumulation of a large number of sugars and organic acids, as well as a depletion of a glycolytic metabolite GAP (Figure 7, B and C). It is not known why and how upregulated defense responses induce such changes in these primary metabolites. It has been reported that sugars can act as ROS scavengers (Keunen et al., 2013). Additionally, glucose, fructose, and sucrose significantly induce the transcription of *Pathogenesis-Related* (*PR*) genes in tobacco (Herbers et al., 1996), and pretreatment of sucrose increases resistance to *Magnaporthe oryzae* infection in rice (Gómez-Ariza et al., 2007). Thus, accumulating more sugars in *los2* mutants may potentially reduce ROS stress and/or amplify immune responses. It is unexpected that the *los2* has reduced PEP but increased SA levels considering that SA is mainly synthesized through shikimate pathway from chorismate which is converted from PEP (Dempsey et al., 2011). However, it is possible that activated immune responses in the *los2* mutant induces a shift of metabolite flux from PEP so that the flux is channeled more to the biosynthesis of SA over some other metabolites despite a reduction of overall PEP. Indeed, it has been shown that enzymes in both the shikimate pathway and the SA biosynthesis pathway are activated at the protein level or induced at gene expression level by pathogen infection or elicitors (Keith et al., 1991; Umeda et al., 1994; Görlach et al., 1995; Ferrari et al., 2007; Yang et al., 2021). Further metabolite analysis will likely reveal the metabolic flux changes in both primary and secondary metabolism with a perturbed glycolysis.

It is not understood how disruption of glycolysis leads to autoimmunity or upregulated defense responses. One hypothesis is that reduced glycolysis reduces energy level and thus reduces pathogen growth. However, similar level of pathogen growth was observed in *los2-5* (with 37% of the WT enolase activity) and *los2-2* alleles (with 10% of the WT enolase activity) (Figure 2, B and F), suggesting that the energy level is not directly related with defense responses. The other hypothesis is that reduced enolase activity perturbs metabolism homeostasis and certain metabolite changes trigger defense responses. Altered levels of some metabolites might induce expression of some NLR genes and therefore activate plant defense responses, and this has been observed for sorbitol in apples (Meng et al., 2018) and plastidial fatty acid in Arabidopsis (Chandra-Shekara et al., 2007). In mammalian cells, an NLR protein complex TLR4-MD-2 can be directly triggered by metabolites lipopolysaccharide and sulfatides (3-*O*-sulfogalactosylceramides) (Park et al., 2009; Su et al., 2021). Although it has not been observed in plants, it is not impossible that one or multiple metabolites altered by the *los2* mutation might activate an NLR protein or a defense response regulator which in turn triggers SA production and upregulates more NLR genes. The NLR gene *SNC1* was shown to be induced by the perturbation of phenylpropanoid metabolism (Huang et al., 2021). It also plays a significant role in conferring autoimmunity in the *los2* mutants (Figure 4, B–D; Supplemental Figure S3C). It is yet to be determined whether *SNC1* or some other NLR genes could be directly activated by a change of metabolites and therefore as a primary sensor in the *los2* mutant or they are induced by SA and therefore as an amplifier of immune response. Future investigation employing metabolomic analysis coupled with molecular genetics will reveal the link between the primary metabolism perturbation and the activation of plant defense responses.

Materials and methods

Plant materials and growth condition

Arabidopsis thaliana accession Col-0 was used as the control for all the experiments performed in this study. Seeds of *los2-2* (SALK_021737), *los2-3* (SALK_077784), and *los2-4* (SAIL_208_E09) were kind gifts from Dr Brigitte Poppenberger (Technical University Munich). For most of the experiments in this study, plants were grown in growth chambers at 22°C under constant light (~100 μmol $m^{-2}s^{-1}$ of fluorescent lamp) and 50% humidity conditions, while plants for pathogen growth assay were grown at 22°C under 12-h light/12-h dark cycle and 50% humidity conditions. Soil (LM111 from Lambert)-grown plants were assayed 2 weeks after germination unless otherwise specified.

Genomic DNA of *LOS2* gene with about 1.5-kb promoter and 600-bp terminator was used for complementation analysis. This DNA fragment was first cloned into pCR8/GW/TOPO vector (Invitrogen, K250020) and then recombined into binary vector pMDC99 by gateway LR clonase (Invitrogen, 11791-020). For *pLOS2:LOS2:GFP*, *pLOS2:ENO2:GFP*, *pLOS2:MBP:GFP*, and *pLOS2:LOS2-S42A:GFP* constructs, an *LOS2* genomic DNA from 1.5-kb upstream of "ATG" site to "TAA" site (without "TAA") was first cloned into pDONR222 vector by gateway BP clonase (Invitrogen, 11789020). The resulting *pLOS2:LOS2*_pDONR222 was used as the template for site mutagenesis by ClonExperess II One Step Cloning kit (Vazyme, C112) or Phusion Site-Directed Mutagenesis Kit (Thermo Scientific, F541) to generate *pLOS2:ENO2*_pDONR222, *pLOS2:MBP*_pDONR222, and *pLOS2:LOS2-S42A*_pDONR222. For constructs *pLOS2:ENO2:NES:YFP* (*ENO2-NES*) and *pLOS2:ENO2:NLS:YFP* (*ENO2-NLS*), *ENO2-NES* and *ENO2-NLS* fusions were made by PCR amplification of the *ENO2* gene with chimeric primers containing the 3′-end of the *ENO2* sequence (right before the stop codon) fused with the NES coding sequences "cttgctcttaagttggctggacttgatatt" or NLS coding sequences "cctaagaagaagagaaaggtt" (see Supplemental Data Set S2). The fusion genes were cloned into pCR8/GW/

TOPO vector and then recombined into gateway binary vector pGWB550 or pGWB540 (Nakagawa et al., 2007). To generate overexpression constructs of *LOS2* variants, the *LOS2* coding region (*LOS2-CDS*) was amplified from WT cDNA and cloned into pDONR222 by gateway BP clonase. The resulting *LOS2-CDS*_pDONR222 was used as a temperate to generate *ENO2-CDS*_pDONR222 by ClonExperess II One Step Cloning kit. The *MBP-CDS* was directly amplified from the second transcription site to the last codon before the stop codon "TAA" and cloned into pDONR222 vector by BP clonase to generate *MBP-CDS*_pDONR222. These entry clones were recombined into gateway binary vector pGWB551 (Nakagawa et al., 2007) or digested by MluI restriction enzyme before recombined into pEarleyGate 103 binary vector by gateway LR clonase. All constructs were sequenced to ensure no PCR errors to cause mutated protein sequences.

Agrobacteria GV3101 (pMP90) strain carrying the desired construct was used for floral dipping to generate transgenic plants. To generate transgenic plants in *los2-4* mutant background, selected transgenic lines in *los2-5* mutant background were crossed with *los2-4* heterozygous plant. Transgenes with *los2-4* homozygous mutant background were isolated in F2 populations by genotyping. Transgenic seeds were screened on 1/2 MS plates with respective antibiotics. T1 plants were transferred into soil from selection plates and grown in the growth chamber for getting T2 seeds. Single-copy transgenic lines were selected by screening T2 seeds on 1/2 MS plates with respective antibiotics, and homozygous plants were identified at T3 generation for these single-copy lines. Experiments were done either on homozygous T3 or T4 plants or on T2 plants that were first selected on 1/2 MS plates with respective antibiotics and were then grown on soil. Primers for making constructs and genotyping can be found in Supplemental Data Set S2.

Mapping-by-sequencing

The cloning of *SMO3* was from the same sequencing analysis as of *SMO1/HOS15* in Yang et al. (2020). Mapping-by-sequencing analysis was performed according to Hua et al. (2017) and Zhu et al. (2012), and further described in Yang et al. (2020).

Pathogen growth assay

Pathogen growth assay in this study was carried out exactly as Yang et al. (2020). Briefly, *Pseudomonas syringae pv. tomato* (*Pst*) DC3000 was grown on King's B medium plates with rifamycin at 28°C for 2 days and re-grown on a new plate for 1 day. Fresh *Pst* DC3000 was suspended in 10-mM $MgCl_2$ and 0.02% Silwet L-77 to OD_{600} of 0.05. Two-week-old plants were dipped in the bacterial suspension for 20 s. Pathogen growth was measured at 1-h or 0 day post-inoculation (0 DPI) and 3 days post-inoculation (3 DPI). Six biological replicates were performed for each analysis.

Gene expression analysis

Two-week-old plants were sampled for total RNA extraction by TRIzol Reagent (Invitrogen, 15596026). cDNA synthesis was performed using PrimeScript RT reagent kit with gDNA eraser (Takara, RR047A). The qRT-PCR reactions were run on CFX96 Real-Time System (Bio-Rad) using iQ SYBR Green supermix (Bio-Rad, 1708880). About two to three individual plants from one pot were pooled as one biological replicate. At least three biological replicates from different pots were performed for each gene expression analysis.

RNA-seq analysis

The RNA-seq analysis of *los2-5* mutant was performed exactly as described in Yang et al. (2020). Three biological replicates were performed for both Col-0 WT and *los2-5* mutants. RNA-seq data of this study can be found at NCBI GEO under the accession number GSE156268. DEGs in *los2-5* mutant with FDR < 0.05 can be found in Supplemental Data Set S1.

3,3′-Diaminobenzidine staining

Two-week-old plants were used for 3,3′-diaminobenzidine (DAB) staining according to Daudi and O'Brien (2012). Briefly, approximately six plants were placed into 50 mL tube with staining solution (1-mg/mL DAB with 0.05% Tween-20) and gently vacuumed for 5 min. Tubes were covered with aluminum foil since DAB is light-sensitive. Tubes were then placed on a shaker at 100 rpm shaking speed until a desired staining was obtained. After incubation, staining solution was replaced with bleaching solution (ethanol: acetic acid: glycerol = 3:1:1) and tubes boiled in a water bath at 90°C for 15 min. Bleaching solution was decanted and replaced with fresh bleaching solution. Samples were allowed to stand for 30 min before plants were photographed on a plain white background under uniform lighting.

Trypan blue staining

The staining solution contained one volume of trypan blue-lactophenol solution (trypan blue at a concentration of 2.5 mg/mL in lactophenol which is a mixture of equal volume of lactic acid, glycerol, phenol, and water) and two volumes of ethanol. At least six 2-week-old plants were immersed in staining solution at room temperature for 1–24 h until desired staining was observed. The staining solution was replaced with bleaching solution (lactophenol: ethanol = 1:2) and the samples were incubated overnight on a shaker at 100 rpm shaking speed. The bleaching solution was removed and the tissue was covered in 70% glycerol. Plants were photographed on a plain white background under uniform lighting.

Immunoblotting

Total protein was extracted from 2-week-old plants (extraction buffer: 50 mM Tris–HCl pH 7.5, 1 mM EDTA, 1 mM EGTA, 150 mM NaCl, 10% glycerol, 5 mM DTT, 0.25% Triton-X 100, 2% Polyvinylpolypyrrolidone, 1 mM PMSF and 1× protease inhibitor cocktail). After separating, proteins were transferred into PVDF membrane (Bio-Rad, 1620177). The anti-GFP antibody (Takara, 632381, at a 1:3,000 dilution) and HRP-linked antibody (Cell Signaling, 7076, at a 1:5,000

dilution) were used as the primary and secondary antibody, respectively, for detecting GFP, YFP and mGFP5 fusion proteins using ECL western blotting detection reagents (GE Healthcare, RPN2209). Membranes were photographed with the Bio-Rad ChemiDoc imaging system.

Dual-luciferase reporter assay

pGreenII 0800-LUC (Hellens et al., 2005) was used as the backbone to generate both effector constructs and the reporter construct. For effectors, *LOS2* CDS was amplified from cDNA of Col-0 WT and Gal4 BD was subcloned from pDEST-GBKT7. DNA fragments were recombined into pGreenII 0800-LUC backbone without renilla and firefly luciferase sequence to generate LOS2-BD_pGreenII0800-LUC and BD_pGreenII0800-LUC by ClonExperess MultiS One Step Cloning kit (Vazyme, C113) or ClonExperess II One Step Cloning kit (Vazyme, C112), respectively. ENO-BD_ pGreenII 0800-LUC and MBP-BD_ pGreenII 0800-LUC were generated using LOS2-BD_ pGreenII 0800-LUC as the temperate by ClonExperess II One Step Cloning kit (Vazyme, C112). In order to generate 5UAS:35S_ pGreenII 0800-LUC, pGreenII 0800-LUC was first digested with PstI and NcoI, then 5UAS (UAS sequence: cggagtactgtcctccgag, from P2-pACU):35S promoter (from pGreen 0800-LUC) with PstI and NcoI restriction site at each end was ligated into the digested backbone by T4 ligation. Ten micrograms of plasmids of one of the effectors and the reporter were co-transformed into Arabidopsis protoplasts. After 16-h incubation in the dark, total RNA in protoplasts was extracted using TRIzol and extracted RNA was subject to cDNA synthesis and subsequent RT-qPCR analyses. Primers used for cloning were listed in Supplemental Data Set S2.

MG132 treatment

Plants were grown on 1/2 MS plates vertically for 1 week in growth chambers at 22°C under constant light and 50% humidity conditions. Seedlings were transferred to six-well tissue culture plates and immersed in 5 mL 1/2 MS liquid medium with 50-μM MG132 (Sigma, M7449). Then the plates were covered with aluminum foil and sited on a shaker with 50 rpm at room temperature. Samples were collected at 0, 1, 4, and 8 h after MG132 treatment, and then subjected to protein extraction and immunoblotting.

Enolase activity measurement

Enolase activity assay in this study was performed following the instructions of Enolase Activity Assay Kit (Sigma, MAK178) with minor modifications. Enolase activity was determined by a couple enzyme assay in which D-2-phosphoglycerate was converted to PEP, resulting in the formation of an intermediate that reacted with a peroxidase substrate. This generated a colorimetric (570 nm) product proportional to the enolase activity in the samples. One milliunit of enolase was the amount of enzyme that generated 1.0 nmole of H_2O_2 per minute at pH 7.2 at 25°C. For sample preparation, 10 mg of 2-week-old plants was homogenized in 100-μL ice-cold enolase assay buffer. Centrifuge the samples at 10,000*g* for 5 min to remove insoluble material and 2 μL of each sample was added into a 96-well plate (Corning Costar, #3696) pre-filled with 23-μL enolase assay buffer in each well. The H_2O_2 standard for colorimetric detection was made by adding 0, 1, 2, 3, 4, 5 μL of the 1 mM H_2O_2 solution into water for a total volume of 25 μL. Then 25 μL reaction mix (21-μL enolase assay buffer, 1-μL enolase substrate mix, 1-μL enolase converter, 1-μL enolase developer, and 1-μL peroxidase substrate) was added into each sample and standard in the well. The 96-well plates with reactions were loaded immediately into a Microplate Reader (BioTek Synergy 2). A blank control with 2 μL of samples, 23-μL enolase assay buffer, and 25-μL reaction mix without the enolase substrate was included for each sample to remove potential background reading not from enolase activity. The microplate reader recorded the measurement every 3 min for 2 h with plates under continuous shaking at 25°C.

Measurement of sugars and organic acids by gas chromatography–mass spectrometry (GC–MS) analysis

The measurement of soluble sugars was performed mainly according to Lisec et al. (2006) as modified by Wang et al. (2010). The whole shoots of 2-week-old soil-grown plants in growth chambers at 22°C under constant light and 50% humidity conditions were sampled. Three individual plants were pooled as one biological replicate and five biological replicates were performed for each genotype. Plant tissues were thoroughly ground in liquid nitrogen, and polar metabolites from 100 mg ground tissue were extracted in 1.4 mL 75% ice-cold methanol, with 60 μL 0.2 mg/mL ribitol added as an internal standard. After fractionation of nonpolar metabolites into chloroform, 30 μL of the aqueous phase was dried under vacuum without heat. The dried sample was derivatized with methoxyamine hydrochloride (Santa Cruz, sc-257710A) and N-methyl-N-trimethylsilyl-trifluoroacetamide (Macherey-Nagel, 701270.110) sequentially for analysis on an Agilent 7890A GC/5975C MS (Agilent Technology, Palo Alto, CA, USA).

Targeted metabolic analysis of glycolytic metabolites and salicylic acid by HPLC-MS

The targeted metabolic analysis for the relative quantitation of glycolytic metabolites and SA was performed using Sciex X500B Q-TOF mass spectrometer coupled with the Exion LC system in Proteomics and Metabolomics facility at Cornell University. The extraction method in this study was performed based on t'Kindt et al. (2008) with the best extracting agent MeOH/H_2O 80/20 as mentioned. Briefly, 50 mg 2-week-old Arabidopsis plants leaves from each genotype were thoroughly ground in liquid nitrogen, and then 250 μL of 2.5 ppm Pyruvic 13C in 80% methanol as an internal standard were added to the homogenized leaf tissues. Sample solutions were vortexed for 10 s at high speed, sonicated for 10 min and then centrifuged to collect supernatant. The sonication step was repeated for the insoluble part

by adding 100 µL of 80% methanol for an additional 10 min, then centrifuging at 16,000*g* for 10 min at room temperature. The resulting supernatant was collected and pooled together. A total of 200 µL supernatant was transferred into a clean tube for each sample and 100 µL of the supernatant filtered using 0.22-µM spin filter (Costar #8169). The filtrate was transferred into autosampler vial and 30 µL of each sample was injected for separation on an HILIC column (100 × 2 mm i.d., 3 µm from Phenomenex). The X500B Q-TOF was operated in negative ion mode under MRM^{HR} method after optimization of MRM parameters for all glycolytic metabolites and SA with their standards. The raw data were acquired and processed using Sciex OS 2.0 software and the relative quantitation of each glycolytic metabolite and SA was determined by integrating the peak areas of each analyte using MRM transitions after normalization against the internal standard Pyruvic 13C.

Statistical analysis

All Student's *t* tests were performed using Excel with $P < 0.05$. The one-way analysis of variation (ANOVA)/Duncan's new multiple range tests were performed using R 3.6.3 with "agricolae" package under $P < 0.05$. Statistical tests and biological replicate numbers were shown in figure legends and methods. Detailed statistical results are provided in Supplemental Data Set S3.

Accession numbers

DNA sequences of all genes in this study were extracted from TAIR with the gene ID listed below: *LOS2* (*AT2G36530*); *SNC1* (*AT4G16890*); *PR1* (*AT2G14610*); *BON1* (*AT5G61900*); *MOS1* (*AT4G24680*); *ZAT10* (*AT1G27730*); *RD29A* (*5G52310*); *COR15A* (*AT2G42540*); *COR47* (*AT1G20440*); *ACTIN2* (*AT3G18780*).

Supplemental Data

The following materials are available in the online version of this article.

Supplemental Figure S1. The *los2* mutants are autoimmune mutants and have defects in enolase activity and development (Supports Figure 2).

Supplemental Figure S2. Total DEGs in *los2-5* mutant and *NahG* transgene rescues the growth defects of *los2-2* mutant (Supports Figure 3).

Supplemental Figure S3. Activated immunity contributes to growth but not developmental defects of *los2* mutant (Supports Figure 4).

Supplemental Figure S4. ENO2 but not MBP rescues the growth defects of *los2* mutants (Supports Figure 5).

Supplemental Figure S5. Protein expression of *pLOS2:LOS2-S42A:GFP* and *pLOS2:ENO2-S42A:GFP* transgenic plants (Supports Figure 6).

Supplemental Figure S6. Enolase activity contributes to the growth regulation of *los2* mutants (Supports Figure 6).

Supplemental Figure S7. Protein expression of different *LOS2* variants in *N. benthamiana* (Supports Figure 8).

Supplemental Figure S8. Transgene and protein expression of complementation lines in *los2-2* mutant (Supports Figure 9).

Supplemental Figure S9. Enolase but not MBP rescues the cold-response gene expression in *los2* mutant. (Supports Figure 9).

Supplemental Data Set S1. Differentially expressed genes (FDR < 0.05) in *los2-5* mutant from RNA-seq.

Supplemental Data Set S2. Primers used in this study.

Supplemental Data Set S3. Summary of statistical analyses.

Acknowledgments

We thank Dr Brigitte Poppenberger for sharing *los2-2*, *los2-3*, and *los2-4* mutant seeds, Dr Chun Han for the 5UAS construct (P2-pACU), Drs Adrienne Roeder, Olena Vatamaniuk, Wei Zhang, Melanie Filiatrault, and Shaoqun Zhou for technical advice and assistance. We thank the Genomics Facility, Bioinformatics Facility, and Imaging Facility of the Biotechnology Resource Center of Cornell Institute of Biotechnology for their assistance and service.

Funding

This work has been supported by National Science Foundation (NSF) IOS-1353738 and IOS-1946174 to J.H.

Conflict of interest statement. None declared.

References

Andriotis VM, Kruger NJ, Pike MJ, Smith AM (2010) Plastidial glycolysis in developing Arabidopsis embryos. New Phytol **185:** 649–662

Bao Z, Zhang N, Hua J (2014) Endopolyploidization and flowering time are antagonistically regulated by checkpoint component MAD1 and immunity modulator MOS1. Nat Commun **5:** 1–10

Barkla BJ, Vera-Estrella R, Hernández-Coronado M, Pantoja O (2009) Quantitative proteomics of the tonoplast reveals a role for glycolytic enzymes in salt tolerance. Plant Cell **21**: 4044–4058

Bechtold U, Ferguson JN, Mullineaux PM (2018) To defend or to grow: lessons from Arabidopsis C24. J Exp Bot **69:** 2809–2821

Bolouri Moghaddam MR, Van den Ende W (2012) Sugars and plant innate immunity. J Exp Bot **63:** 3989–3998

Bolton MD (2009) Primary metabolism and plant defense—fuel for the fire. Mol Plant-Microbe Interact **22**: 487–497

Boukouris AE, Zervopoulos SD, Michelakis ED (2016) Metabolic enzymes moonlighting in the nucleus: metabolic regulation of gene transcription. Trends Biochem Sci **41:** 712–730

Buscaill P, Rivas S (2014) Transcriptional control of plant defence responses. Curr Opin Plant Biol **20:** 35–46

Chandra-Shekara AC, Venugopal SC, Barman SR, Kachroo A, Kachroo P (2007) Plastidial fatty acid levels regulate resistance gene-dependent defense signaling in Arabidopsis. Proc Natl Acad Sci USA **104:** 7277–7282

Chisholm ST, Coaker G, Day B, Staskawicz BJ (2006) Host-microbe interactions: shaping the evolution of the plant immune response. Cell **124:** 803–814

Couto D, Zipfel C (2016) Regulation of pattern recognition receptor signalling in plants. Nat Rev Immunol **16:** 537

Cui H, Gobbato E, Kracher B, Qiu J, Bautor J, Parker JE (2017) A core function of EDS1 with PAD4 is to protect the salicylic acid

defense sector in Arabidopsis immunity. New Phytol **213:** 1802–1817

Cui H, Tsuda K, Parker JE (2015) Effector-triggered immunity: from pathogen perception to robust defense. Annu Rev Plant Biol **66:** 487–511

Daudi A, O'Brien JA (2012) Detection of hydrogen peroxide by DAB staining in Arabidopsis leaves. Bio-protocol **2:** e263

Delaney TP, Uknes S, Vernooij B, Friedrich L, Weymann K, Negrotto D, Gaffney T, Gut-Rella M, Kessmann H, Ward E, et al. (1994) A central role of salicylic acid in plant disease resistance. Science **266:** 1247–1250

Dempsey DMA, Vlot AC, Wildermuth MC, Klessig DF (2011) Salicylic acid biosynthesis and metabolism. The Arabidopsis Book **9:** e0156

Didiasova M, Schaefer L, Wygrecka M (2019) When place matters: shuttling of enolase-1 across cellular compartments. Front Cell Dev Biol **7:** 61

Eremina M, Rozhon W, Yang S, Poppenberger B (2015) ENO 2 activity is required for the development and reproductive success of plants, and is feedback-repressed by At MBP-1. Plant J **81:** 895–906

Feo S, Arcuri D, Piddini E, Passantino R, Giallongo A (2000) ENO1 gene product binds to the c-myc promoter and acts as a transcriptional repressor: relationship with Myc promoter-binding protein 1 (MBP-1). FEBS Lett **473:** 47–52

Ferrari S, Galletti R, Denoux C, De Lorenzo G, Ausubel FM, Dewdney J (2007) Resistance to *Botrytis cinerea* induced in Arabidopsis by elicitors is independent of salicylic acid, ethylene, or jasmonate signaling but requires PHYTOALEXIN DEFICIENT3. Plant Physiol **144:** 367–379

Gebauer P, Korn M, Engelsdorf T, Sonnewald U, Koch C, Voll LM (2017) Sugar accumulation in leaves of Arabidopsis sweet11/-sweet12 double mutants enhances priming of the salicylic acid-mediated defense response. Front Plant Sci **8:** 1378

Glawischnig E (2007) Camalexin. Phytochemistry **68:** 401–406

Gómez-Ariza J, Campo S, Rufat M, Estopà M, Messeguer J, Segundo BS, Coca M (2007) Sucrose-mediated priming of plant defense responses and broad-spectrum disease resistance by overexpression of the maize pathogenesis-related PRms protein in rice plants. Mol Plant-Microbe Interact **20:** 832–842

Görlach J, Raesecke HR, Rentsch D, Regenass M, RoY P, Zala M, Keel C, Boller T, Amrhein N, Schmid J (1995) Temporally distinct accumulation of transcripts encoding enzymes of the prechorismate pathway in elicitor-treated, cultured tomato cells. Proc Natl Acad Sci USA **92:** 3166–3170

Hellens RP, Allan AC, Friel EN, Bolitho K, Grafton K, Templeton MD, Karunairetnam S, Gleave AP, Laing WA (2005) Transient expression vectors for functional genomics, quantification of promoter activity and RNA silencing in plants. Plant Methods **1:** 1–14

Herbers K, Meuwly P, Métraux JP, Sonnewald U (1996) Salicylic acid-independent induction of pathogenesis-related protein transcripts by sugars is dependent on leaf developmental stage. FEBS Lett **397:** 239–244

Hua J, Wang S, Sun Q (2017) Mapping and cloning of chemical induced mutations by whole-genome sequencing of bulked segregants. *In* Plant Pattern Recognition Receptors. Humana Press, New York, pp 285–289

Huang XX, Wang Y, Lin JS, Chen L, Li YJ, Liu Q, Wang G-F, Xu F, Liu L, Hou BK (2021) The novel pathogen-responsive glycosyltransferase UGT73C7 mediates the redirection of phenylpropanoid metabolism and promotes SNC1-dependent Arabidopsis immunity. Plant J **107:** 149–165

Jones JD, Dangl JL (2006) The plant immune system. Nature **444:** 323–329

Kang HJ, Jung SK, Kim SJ, Chung SJ (2008) Structure of human α-enolase (hENO1), a multifunctional glycolytic enzyme. Acta Crystallogr D Biol Crystallogr **64:** 651–657

Kang M, Abdelmageed H, Lee S, Reichert A, Mysore KS, Allen RD (2013) At MBP-1, an alternative translation product of LOS2, affects abscisic acid responses and is modulated by the E3 ubiquitin ligase AtSAP5. Plant J **76:** 481–493

Keith B, Dong XN, Ausubel FM, Fink GR (1991) Differential induction of 3-deoxy-D-arabino-heptulosonate 7-phosphate synthase genes in *Arabidopsis thaliana* by wounding and pathogenic attack. Proc Natl Acad Sci USA **88:** 8821–8825

Keunen ELS, Peshev D, Vangronsveld J, Van Den Ende WIM, Cuypers ANN (2013) Plant sugars are crucial players in the oxidative challenge during abiotic stress: extending the traditional concept. Plant Cell Environ **36:** 1242–1255

Kim JW, Dang CV (2005) Multifaceted roles of glycolytic enzymes. Trends Biochem Sci **30:** 142–150

Lapin D, Bhandari DD, Parker JE (2020) Origins and immunity networking functions of EDS1 family proteins. Annu Rev Phytopathol **58:** 253–276

Lee H, Guo Y, Ohta M, Xiong L, Stevenson B, Zhu JK (2002) *LOS2*, a genetic locus required for cold-responsive gene transcription encodes a bi-functional enolase. EMBO J **21**: 2692–2702

Lisec J, Schauer N, Kopka J, Willmitzer L, Fernie AR (2006) Gas chromatography mass spectrometry–based metabolite profiling in plants. Nat Protoc **1:** 387–396

Liu X, Wei W, Zhu W, Su L, Xiong Z, Zhou M, Zheng Y, Zhou DX (2017) Histone deacetylase AtSRT1 links metabolic flux and stress response in Arabidopsis. Mol Plant **10:** 1510–1522

Lolle S, Stevens D, Coaker G (2020) Plant NLR-triggered immunity: from receptor activation to downstream signaling. Curr Opin Immunol **62:** 99–105.

Lung J, Liu KJ, Chang JY, Leu SJ, Shih NY (2010) MBP-1 is efficiently encoded by an alternative transcript of the ENO1 gene but post-translationally regulated by proteasome-dependent protein turnover. FEBS J **277:** 4308–4321

Meng D, Li C, Park HJ, González J, Wang J, Dandekar AM, Turgeon G, Cheng L (2018) Sorbitol modulates resistance to *Alternaria alternata* by regulating the expression of an NLR resistance gene in apple. Plant Cell **30:** 1562–1581

Meyers BC, Kozik A, Griego A, Kuang H, Michelmore RW (2003) Genome-wide analysis of NBS-LRR–encoding genes in Arabidopsis. Plant Cell **15:** 809–834

Morkunas I, Ratajczak L (2014) The role of sugar signaling in plant defense responses against fungal pathogens. Acta Physiol Plant **36:** 1607–1619

Nakagawa T, Suzuki T, Murata S, Nakamura S, Hino T, Maeo K, Tabata R, Kawai T, Tanaka K, Niwa Y, et al. (2007) Improved gateway binary vectors: high-performance vectors for creation of fusion constructs in transgenic analysis of plants. Biosci Biotechnol Biochem **71:** 2095–2100

Návarová H, Bernsdorff F, Döring AC, Zeier J (2012) Pipecolic acid, an endogenous mediator of defense amplification and priming, is a critical regulator of inducible plant immunity. Plant Cell **24:** 5123–5141

Pancholi V (2001) Multifunctional α-enolase: its role in diseases. Cell Mol Life Sci CMLS, **58:** 902–920

Park BS, Song DH, Kim HM, Choi BS, Lee H, Lee JO (2009) The structural basis of lipopolysaccharide recognition by the TLR4–MD-2 complex. Nature **458:** 1191–1195

Piasecka A, Jedrzejczak-Rey N, Bednarek P (2015) Secondary metabolites in plant innate immunity: conserved function of divergent chemicals. New Phytol **206:** 948–964

Plaxton WC (1996) The organization and regulation of plant glycolysis. Annu Rev Plant Biol **47:** 185–214

Prabhakar V, Löttgert T, Geimer S, Dörmann P, Krüger S, Vijayakumar V, Schreiber L, Gobel C, Feussner K, Feussner I, et al. (2010) Phosphoenolpyruvate provision to plastids is essential for gametophyte and sporophyte development in *Arabidopsis thaliana*. Plant Cell **22:** 2594–2617

Ray R, Miller, DM (1991) Cloning and characterization of a human c-myc promoter-binding protein. Mol Cell Biol **11:** 2154–2161

Rius SP, Casati P, Iglesias AA, Gomez-Casati DF (2008) Characterization of Arabidopsis lines deficient in GAPC-1, a cytosolic NAD-dependent glyceraldehyde-3-phosphate dehydrogenase. Plant Physiol **148:** 1655–1667

Rodríguez A, Cera TDL, Herrero P, Moreno F (2001) The hexokinase 2 protein regulates the expression of the *GLK1*, *HXK1* and *HXK2* genes of *Saccharomyces cerevisiae*. Biochem J **355:** 625–631

Saijo Y, Loo EPI (2020) Plant immunity in signal integration between biotic and abiotic stress responses. New Phytol **225:** 87–104

Shah J, Chaturvedi R, Chowdhury Z, Venables B, Petros RA (2014) Signaling by small metabolites in systemic acquired resistance. Plant J **79:** 645–658

Shams F, Oldfield NJ, Wooldridge KG, Turner DP (2014) Fructose-1, 6-bisphosphate aldolase (FBA)–a conserved glycolytic enzyme with virulence functions in bacteria: 'Ill met by moonlight'. Biochem Soc Trans **42:** 1792–1795

Su L, Athamna M, Wang Y, Wang J, Freudenberg M, Yue T, Wang J, Moresco EMY, He H, Zor T, et al. (2021) Sulfatides are endogenous ligands for the TLR4–MD-2 complex. Proc Natl Acad Sci USA **118**: e2105316118

Tang D, Wang G, Zhou JM (2017) Receptor kinases in plant-pathogen interactions: more than pattern recognition. Plant Cell **29:** 618–637

t'Kindt R, Veylder LD, Storme M, Deforce D, Bocxlaer JV (2008) LC-MS metabolic profilin of *Arabidopsis thaliana* plant leaves and cell cultures: optimization of pre-LC-MS procedure parameters. J Chromatogr B **871:** 37–43

Trouvelot S, Héloir MC, Poinssot B, Gauthier A, Paris F, Guillier C, Combier M, Trda L, Daire X, Adrian M (2014) Carbohydrates in plant immunity and plant protection: roles and potential application as foliar sprays. Front Plant Sci **5:** 592

Umeda M, Hara C, Matsubayashi Y, Li HH, Liu Q, Tadokoro F, Aotsuka S, Uchimiya H (1994) Expressed sequence tags from cultured cells of rice (*Oryza sativa* L.) under stressed conditions: analysis of transcripts of genes engaged in ATP-generating pathways. Plant Mol Biol **25:** 469–478

Wang H, Ma F, Cheng L (2010) Metabolism of organic acids, nitrogen and amino acids in chlorotic leaves of 'Honeycrisp' apple (*Malus domestica* Borkh) with excessive accumulation of carbohydrates. Planta **232:** 511–522

Yang L, Chen X, Wang Z, Sun Q, Hong A, Zhang A, Zhong X, Hua J (2020) HOS15 and HDA9 negatively regulate immunity through histone deacetylation of intracellular immune receptor NLR genes in Arabidopsis. New Phytol **226:** 507–522

Yang L, Wang Z, Hua J (2021) A meta-analysis reveals opposite effects of biotic and abiotic stresses on transcript levels of Arabidopsis intracellular immune receptor genes. Front Plant Sci **12**: 241

Yang S, Hua J (2004) A haplotype-specific resistance gene regulated by BONZAI1 mediates temperature-dependent growth control in Arabidopsis. Plant Cell **16:** 1060–1071

Zhao Z, Assmann SM (2011) The glycolytic enzyme, phosphoglycerate mutase, has critical roles in stomatal movement, vegetative growth, and pollen production in *Arabidopsis thaliana*. J Exp Bot **62:** 5179–5189

Zheng L, Roeder RG, Luo Y (2003) S phase activation of the histone H2B promoter by OCA-S, a coactivator complex that contains GAPDH as a key component. Cell **114:** 255–266

Zhu Y, Mang HG, Sun Q, Qian J, Hipps A, Hua J (2012) Gene discovery using mutagen-induced polymorphisms and deep sequencing: application to plant disease resistance. Genetics **192:** 139–146